Quaternary Science Reviews 268 (2021) 107108

Contents lists available at ScienceDirect

Quaternary Science Reviews

journal homepage: www.elsevier.com/locate/quascirev

Meltwater flux from northern ice-sheets to the mediterranean during MIS 12

Lucía A. Azibeiro [a, *], Francisco J. Sierro [a], Lucilla Capotondi [b], Fabrizio Lirer [c], Nils Andersen [d], Alba González-Lanchas [a], Montserrat Alonso-Garcia [a], José-Abel Flores [a], Aleix Cortina [e], Joan O. Grimalt [e], Belen Martrat [e], Isabel Cacho [f]

[a] Department of Geology, University of Salamanca, 37008, Salamanca, Spain
[b] CNR, Istituto di Scienze Marine (ISMAR), Via Gobeti 101, 40129, Bologna, Italy
[c] CNR, Istituto di Scienze Marine (ISMAR), 80133, Napoli, Italy
[d] Leibniz-Laboratory for Radiometric Dating and Isotope Research, Christian-Albrechts-Universität zu Kiel, Kiel, Germany
[e] Department of Environmental Chemistry, IDAEA-CSIC, 08034, Barcelona, Spain
[f] GRC Geociències Marines, Departament de Dinàmica de la Terra i de l'Oceà, Facultat de Ciències de la Terra, Universitat de Barcelona, 08028, Barcelona, Spain

ARTICLE INFO

Article history:
Received 3 May 2021
Received in revised form
21 July 2021
Accepted 22 July 2021
Available online 12 August 2021

Handling Editor: Dr A. Voelker

Keywords:
Mediterranean
Millennial climate variability
Freshwater
Meltwater
Palaeoceanography
Marine isotope stage 12
Foraminifera
Glacial

ABSTRACT

Planktonic foraminifer oxygen isotopes through MIS 12 were analysed from Ocean Drilling Program Site 977 in the Alboran Sea. After the correction of the sea surface temperature (SST) effect on the $\delta^{18}O$ composition of foraminiferal calcite, the resulting seawater $\delta^{18}O$ ($\delta^{18}O_w$) was used to reconstruct variations in the $\delta^{18}O_w$ of the Atlantic inflow into the Mediterranean. A synchronous record from the KC01B core, in the Ionian Sea, was used to evaluate changes in the oxygen isotope gradient within the Mediterranean due to hydrological variations during MIS 12. Instead of the glacial $\delta^{18}O_w$ enrichment expected for the Mediterranean, lower values than today have been observed both in the Alboran and the Ionian seas, especially between 455 ka and the end of MIS 12 (424 ka). These negative oxygen isotope anomalies must have been caused by a flux of freshwater to the Mediterranean during MIS 12. Although the largest fraction of the freshwater anomalies entered the Mediterranean through the Atlantic inflow, especially during Heinrich stadials, the Mediterranean $\delta^{18}O_w$ gradient allowed us to identify other sources of freshwater to the eastern basin. One of these sources was probably the meltwater generated at the southern margin of the Fennoscandian ice-sheet that entered via the Caspian and Black seas. However, the proximity of core KC01B to the Adriatic Sea points to meltwater delivered from the Alpine ice-sheet and transported through the Po river into the Mediterranean as the main cause of the Ionian Sea ^{18}O depletions.

1. Introduction

Sea surface salinity and oxygen isotope composition of the Mediterranean water changed at millennial and orbital time scales (e.g. Cacho et al., 1999; Cacho et al., 2000; Capotondi et al., 2016; Grant et al., 2016; Jiménez-Amat and Zahn, 2015; Marino et al., 2018; Sierro et al., 2005). Episodes of surface $\delta^{18}O$ depletions have been related to freshening events triggered by meltwater entries from the Atlantic. Most of these episodes have been associated with the so-called Heinrich events (HE) during some of the coldest stadials and involved iceberg calving in the Atlantic margin from Laurentide and Eurasian ice-sheets (Bond et al., 1992, 1993; Broecker et al., 1992; Grousset et al., 2000; Heinrich, 1988). The meltwater release into the high latitudes of the Atlantic decreased the advection of subtropical waters due to slowdown of North Atlantic Deep Water (NADW) formation and triggered the southward migration of the polar front (Barker et al., 2015; Bond et al., 1993, 1999; Broecker et al., 1985, 1992; Cacho et al., 1999, 2001; Elliot et al., 2002; Hodell et al., 2017; McManus et al., 2004; Peck et al., 2006; Vidal et al., 1997). Although current north-eastern Atlantic circulation promotes a major advection of the subtropical salty water of the Azores Current (AzC) into the Gulf of Cadiz (Peliz

* Corresponding author.
E-mail address: LuciaAA@usal.es (L.A. Azibeiro).

https://doi.org/10.1016/j.quascirev.2021.107108

et al., 2005), a higher prevalence of the southward less salty and cooler water of the Portugal Current has been reported during these episodes of deep Atlantic circulation slowdown. This predominant northern impact favours the advection of icebergs to the southern Iberian Margin and the meltwater flow into the Mediterranean (e.g. Cacho et al., 1999; Cacho et al., 2000; Capotondi et al., 2016; Girone et al., 2013; Marino et al., 2018; Palumbo et al., 2013; Sierro et al., 2020; Sierro et al., 2005; Voelker et al., 2009).

The most extensive glaciation over the last 500 ka ended with a pronounced long deglaciation that culminated in one of the longest interglacials (MIS 11) (Bauch and Erlenkeuser, 2003; Ehlers and Gibbard, 2004; Jouzel et al., 2007; Lisiecki and Raymo, 2005; Naafs et al., 2014; Poli et al., 2000; Rohling et al., 1998a, 2014; Stein et al., 2009; Toucanne et al., 2009; Tzedakis et al., 2006, 2012). During MIS 12, the European ice-sheet reached the maximum extent of the last 1.2 Ma (Toucanne et al., 2009) and this huge amount of continental ice was lost during the deglaciation, thus producing a large freshwater entry to the Atlantic and potentially propagating to the Mediterranean.

Changes in the Mediterranean hydrologic budget along the Pleistocene and Holocene have been related to variations in evaporation or, more frequently, to varying entries of freshwater from different sources such as the Nile, the Black Sea or the mightiest rivers from the northern margin (Lane-Serff et al., 1997; Rossignol-Strick, 1985; Rossignol-Strick et al., 1982; Ryan et al., 1997, 2003; Sperling et al., 2003; Vidal et al., 2010). These intra-basin freshwater discharges had an important impact on the Mediterranean hydrologic budget that substantially changed the seawater $\delta^{18}O$ ($\delta^{18}O_w$) and salinity of the Atlantic inflow along its path to the eastern basin. Studies of the east Mediterranean oxygen isotope stack (Lourens, 2004; Rohling et al., 2014; Wang et al., 2010) detected great ^{18}O depletions during MIS 12, 14 and 16 explained by hypothetical extra freshwater input into the Mediterranean during these major glaciations.

The main objective of the present study was the characterization of meltwater flux from the northern ice-sheets to the Mediterranean during MIS 12. Through the study of planktonic foraminiferal oxygen isotope data from the Alboran and Ionian seas and the estimation of SST in both, we attempted to reconstruct variations in the oxygen isotope composition of the Atlantic inflow and the impact of variations in the Mediterranean hydrology on the $\delta^{18}O_w$ along its path to the eastern basin. This study highlights the contribution of the Alpine ice-sheet during episodes of ^{18}O depletions in the Ionian Sea.

2. Modern mediterranean sea surface salinity and $\delta^{18}O$

The Mediterranean is a semienclosed sea with a hydrologic regime characterized by excess of evaporation over freshwater input (precipitation and runoff) (Bethoux, 1979; Lacombe, 1981). As a consequence, there is an Atlantic surface water inflow that compensates the evaporative loss and the Mediterranean outflow, generating an anti-estuarine circulation system. The comparatively low saline Atlantic water flows over the underlaying Mediterranean saltier water and mixes in the Alboran Sea to form the modified Atlantic water (MAW) that moves eastward along the African coast and penetrates the eastern Mediterranean through the Strait of Sicily (Fig. 1a) (Font et al., 1998; Millot, 1999). The exposure of the MAW to the negative hydrologic budget toward the east, results in a longitudinal salinity gradient (Fig. 1a) until the buoyancy loss, linked to the high salinity in the east, force the surface water to sink to intermediate depth. As a result the Levantine intermediate water is formed and returns to Gibraltar until its exit to the Atlantic (Bethoux, 1979; Dämmer et al., 2020; Emelianov et al., 2006; Lacombe, 1981; Millot and Taupier-Letage, 2005).

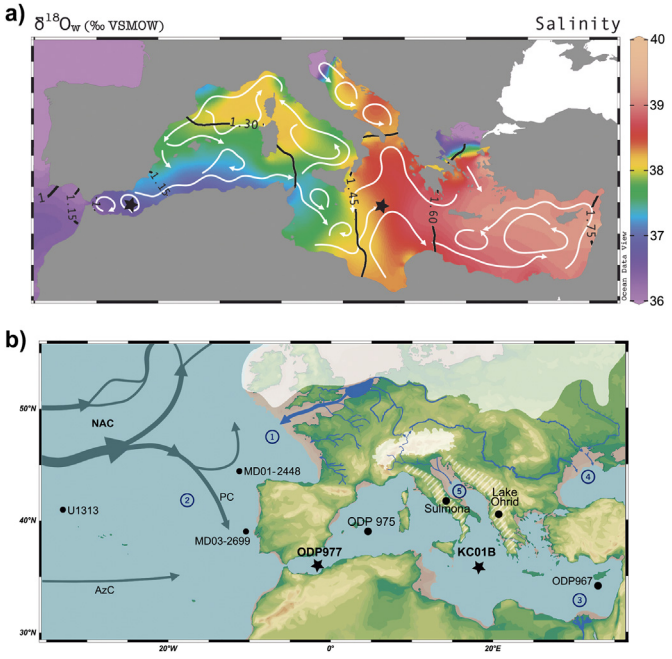

Fig. 1. a) Sea Surface Salinity in colours (Zweng et al., 2018 (WOA, 1998)) and $\delta^{18}O_w$ isolines (black lines) (LeGrande and Schmidt, 2006; Pierre, 1999) with ODP Site 977 and KC01B locations. The white lines indicate the main surface currents (Macias et al., 2019). b) Location of the studied sites ODP 977 and KC01B, and the main sites mentioned throughout this study. White areas display approximate British, Scandinavian and Alpine ice-sheets extension during MIS 12 (Batchelor et al., 2019; Ehlers and Gibbard, 2004). The white striped areas display Apennine, Dinaric Alps and Pindus Mountains areas where small ice caps could have occurred (Hughes et al., 2010, 2011; Woodward et al., 2008). Dark arrows in the Atlantic delineate the main surface currents mentioned in this study: North Atlantic Current (NAC), Azores Current (AzC) and the Portugal Current (PC) (Daniault et al., 2016; Toucanne et al., 2021). The blue lines on the continent illustrate drainage systems that represent potential freshwater sources: (1) Fleuve Manche, and drainage of Loire and Gironde rivers (Toucanne et al., 2009) that could have joined the Laurentide meltwaters in the (2) PC. (3) Nile river discharge to the eastern Mediterranean, (4) Danube, Dniester and Dnieper rivers into the Black Sea and (5) Po river drainage to the Adriatic Sea (Martinez-Lamas et al., 2020). Light brown areas represent the approximate shoreline paleogeography for 120 m of sea level lowstand with no compensation for uplift or subsidence of the coastline. The software Ocean Data View (Schlitzer, R., Ocean Data View, odv. awi.de, 2018) was used to generate this figure. (For interpretation of the references to colour in this figure legend, the reader is referred to the Web version of this article.)

Both $\delta^{18}O_w$ and salinity are water budget dependent and correlated in the modern Mediterranean (Fig. 1a), however, variations in both properties are not linearly correlated. Mediterranean salinity is a function of the volume flux of the Atlantic inflow, its salinity and the Mediterranean net freshwater flux. Meanwhile, Mediterranean $\delta^{18}O_w$ depends on the volume flux of the Atlantic inflow, its $\delta^{18}O_w$ and the O-isotope mass balanced mean of the different freshwater inputs and of the evaporated water (see Rohling, 2007) which generates the observed $\delta^{18}O_w$ longitudinal gradient along the Mediterranean.

As a result, the Atlantic inflow with an average $\delta^{18}O_w$ of 1‰ and salinity of 36.2, increases up to 1.75‰ and 39.4 in the easternmost Mediterranean (LeGrande and Schmidt, 2006; Pierre, 1999; Zweng et al., 2018). Mixing at the Strait of Gibraltar today only causes a minor change in the Atlantic inflow $\delta^{18}O_w$ as may be inferred from similar $\delta^{18}O_w$ at both sides of the strait (LeGrande and Schmidt, 2006; Schmidt, 1999; Pierre, 1999; Voelker et al., 2015). Due to the location of Ocean Drilling Program (ODP) Site 977 (ODP Site 977) close to Strait of Gibraltar (Fig. 1 a and b), the surface $\delta^{18}O_w$ at this location mainly reflects the $\delta^{18}O_w$ of the Atlantic inflow registering the freshwater perturbations occurring in the Atlantic

and propagated into the Mediterranean Sea. At the location of core KC01B in the Ionian Sea, average values of 1.47‰ and 38.3 are observed today. A gradient of 0.38‰ in the $\delta^{18}O_w$ and 1.4 in salinity is recorded today between surface water at sites ODP 977 and KC01B.

3. Materials and methods

$\delta^{18}O$ planktonic foraminiferal records from two Mediterranean cores were compared in this study: ODP Site 977 and KC01B (Fig. 1). ODP 977 (36°01.907′N, 1°57.319′W) was recovered from a water depth of 1984 m south of Cabo de Gata (Eastern Alboran Sea) and sampled every 5 cm on average from 64.09 to 71.99 m. A total of 146 samples were analysed for this study (~468 yr average time resolution based on the age model discussed below). The sediment, which is composed of calcareous clay and nannofossil ooze (Comas et al., 1996), constitutes a continuous record validated by previous studies (González-Lanchas et al., 2020; Marino et al., 2018; Martrat et al., 2004; Pérez-Folgado et al., 2003, 2004). Site KC01B (36°15.250′ N, 17°44.340′ E) (Fig. 1) was recovered on the Pisano Plateau (southern Calabrian Ridge, Ionian Sea), during MD69 cruise of the R/V Marion Dufresne from 3643 m water depth. We analysed samples previously studied in Capotondi et al. (2016) with an average resolution of 4 cm from 19.1 to 20.5 m (~1260 ka resolution).

Samples were washed with deionized water over a 63 μm sieve and residues were dried and sieved again through a 150 μm sieve. The size fraction >150 μm was split to obtain an aliquot of ~300 planktonic foraminifer specimens. In order to compare foraminiferal data from the same size fraction, we performed an additional counting for Site KC01B to that published by Capotondi et al. (2016), using the size fraction >150 μm. Relative abundances of all species were calculated to estimate sea surface temperature (SST) with the 10 transfer functions derived from backpropagating artificial neural network (ANN) (Malmgren et al., 2001) trained with the (Kucera et al., 2005) Mediterranean coretop dataset.

Around 11 specimens of *Globigerina bulloides* from the 300–355 μm size fraction were picked to obtain the $\delta^{18}O$ record of ODP 977 using a Thermo-Finnigan MAT-252 mass spectrometer at the University of Barcelona as described in González-Lanchas et al. (2020). Oxygen isotopes were also measured in approximately 10 specimens of *Neogloboquadrina incompta* from the >150 μm fraction after organic matter removal by soaking in 15% H_2O_2 and ultrasound cleaning with methanol. The $\delta^{18}O$ measurements were performed on a Thermo-Finnigan MAT 253 mass spectrometer coupled to a Kiel IV carbonate preparation device at the Leibniz Laboratory for Radiometric Dating and Isotope Research of the Christian-Albrechts University in Kiel. The analytical precision of two international standards (NBS-19; IAEA-603) and three laboratory internal standards was better than ±0.08‰. Results are reported relative to the Vienna Pee Dee Belemnite (VPDB) scale. Oxygen isotopes from *N. incompta* were measured to obtain a record comparable to that of the Ionian Sea published by Capotondi et al. (2016).

3.1. Surface seawater oxygen isotope estimation

To estimate past $\delta^{18}O_w$ at ODP Site 977, we first established the relation between the recent $\delta^{18}O_w$ at this location (1.09‰, LeGrande and Schmidt, 2006; Pierre, 1999) and the $\delta^{18}O$ of *N. incompta* today (1.20 ± 0.11‰ from the last 3 ka at ODP Site 977 and the nearby core MD95-2043). *N. incompta* has been reported to dwell in subsurface waters in the Mediterranean (Rohling et al., 2004). If *N. incompta* precipitates its shells today in isotope equilibrium with seawater, the temperature of precipitation should be ~16 °C using the equation of Erez and Luz (1983) which approximately coincides with a water depth shallower than 100 m. This water depth corresponds to the MAW, assuming there is no vital effect. This temperature is close to winter-spring SST at ODP Site 977 (15.88 ± 0.31 °C, WOA, 1998). Based on this, we estimated past $\delta^{18}O_w$ during MIS 12 by adding to the present $\delta^{18}O_w$ the effect of the winter SST change relative to present on the foraminifers calcite $\delta^{18}O$ values (Kim and O'Neil, 1997) using the winter SST calculated with the ANN methodology. Although the vital effect for *N. incompta* is unknown in the Mediterranean, a similar effect was assumed for both sites. Additionally, the ice volume effect on the calcite $\delta^{18}O$ was also removed using the sea level record of Grant et al. (2014) and a ratio of 0.008‰ per m of sea level (Lea et al., 2002).

No recent $\delta^{18}O$ measurement for *N. incompta* is available for KC01B. Then, assuming similar dwelling conditions for *N. incompta* in the Ionian Sea, living near the Deep Chlorophyll Maximum (DCM) in the base of the euphotic layer (Casford et al., 2003; Grant et al., 2016; Rohling et al., 2004) and the same isotopic equilibrium, we estimated a calcite $\delta^{18}O$ value of 1.32‰ from current values of 16.10 °C and $\delta^{18}O_w$ of 1.47‰ (Boyer et al., 2018; LeGrande and Schmidt, 2006; Pierre, 1999). KC01B $\delta^{18}O_w$ during MIS 12 was calculated as previously described for ODP 977. The oxygen isotopic relationship between VSMOW (Vienna-Standard Mean Ocean Water) and VPDB scales was taken from Kim et al. (2015) (modified from Coplen et al., 1983; Craig, 1957).

To reconstruct the Mediterranean longitudinal $\delta^{18}O_w$ gradient, a common time scale with a constant step of 1 ka was obtained by interpolating ODP 977 and KC01B records. The gradient was calculated as [(KC01B $\delta^{18}O_w$) − (ODP 977 $\delta^{18}O_w$)].

3.2. Age model

In order to construct the chronology for ODP Site 977, SST changes in the NE Atlantic at mid latitude and western Mediterranean were considered synchronous because the two areas were connected with the same surface ocean circulation in the late Pleistocene (Artale et al., 2006; Cacho et al., 1999; Myers et al., 1998; Paterne et al., 1999; Rogerson et al., 2008, 2010; Rohling et al., 1998b) and during the MIS 12 and MIS 11 (Girone et al., 2013; Kandiano et al., 2012; Voelker et al., 2010). Based on this assumption, we built an age model for ODP Site 977 by aligning its alkenone-based SST record (extended from González-Lanchas et al., 2020) to that of the north Atlantic mid-latitude record IODP Site U1313 (Naafs et al., 2011; Stein et al., 2009) (Fig. 2). Two primary control points for MIS 12 were added to extend the age model of González-Lanchas et al. (2020).

The existing KC01B age model was elaborated through the tuning of sapropels with the astronomical records (Capotondi et al., 2016; Konijnendijk et al., 2014; Lourens, 2004). An age model based on the Lisiecki and Raymo (2005) global benthic stack was performed for KC01B in this study using the ODP Site 977 previously described chronology as target. As observed in previous studies of the western Mediterranean, the $\delta^{18}O$ measurements obtained from *G. bulloides* show high correlation with the *N. incompta* records, although *G. bulloides* $\delta^{18}O$ signal shows higher short-term variability (Grant et al., 2016) (Fig. 3). Rohling et al. (2004) associated this dissimilitude with differences in depth habitats and seasonal growth. Then, the subsurface dwelling species *N. incompta* gives a more stable signal, but similar to that of *G. bulloides*. Because of this, $\delta^{18}O$ measurements in *N. incompta* from ODP Site 977 and KC01B were synchronized for MIS 12 and early MIS 11 while *G. bulloides* $\delta^{18}O$ record from ODP Site 977 was used for younger ages (Fig. 3). With this proposed age model, the timing of tephra I24 (Lourens, 2004) is established ca. 458 ka, which matches within dating

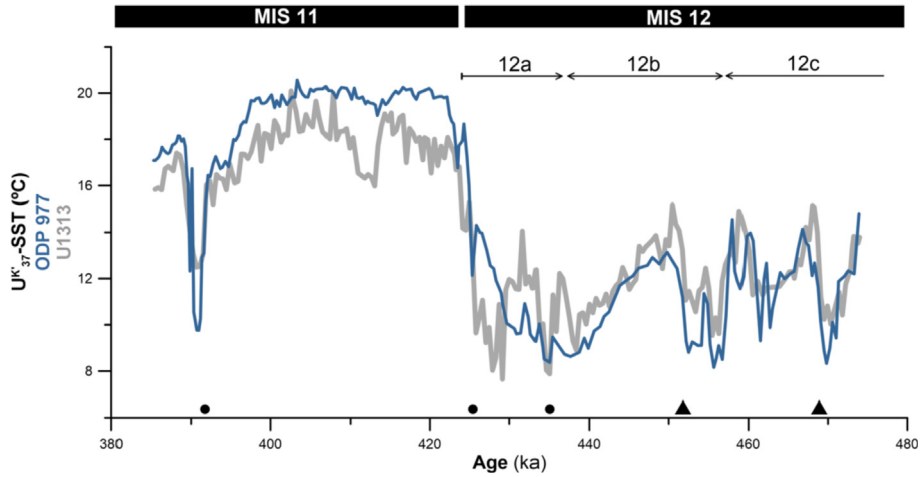

Fig. 2. Age model of the studied interval performed by correlating alkenone-derived SST from ODP Site 977 (blue) with U1313 (grey) (Naafs et al., 2011; Stein et al., 2009) LR04-based chronology (Lisiecki and Raymo, 2005). The dots over the time axis (ka) indicate González-Lanchas et al. (2020) tie points while triangles are primary control points used in this study to extend the tuning for MIS 12. Substages MIS 12a, 12b and 12c nomenclature was adopted from Railsback et al. (2015), i.e., MIS 12c (~478–457 ka), 12b (~457–437ka) and 12a (~437–424 ka). The boundary between MIS 12 and MIS 11 was adopted from Lisiecki and Raymo (2005). (For interpretation of the references to colour in this figure legend, the reader is referred to the Web version of this article.)

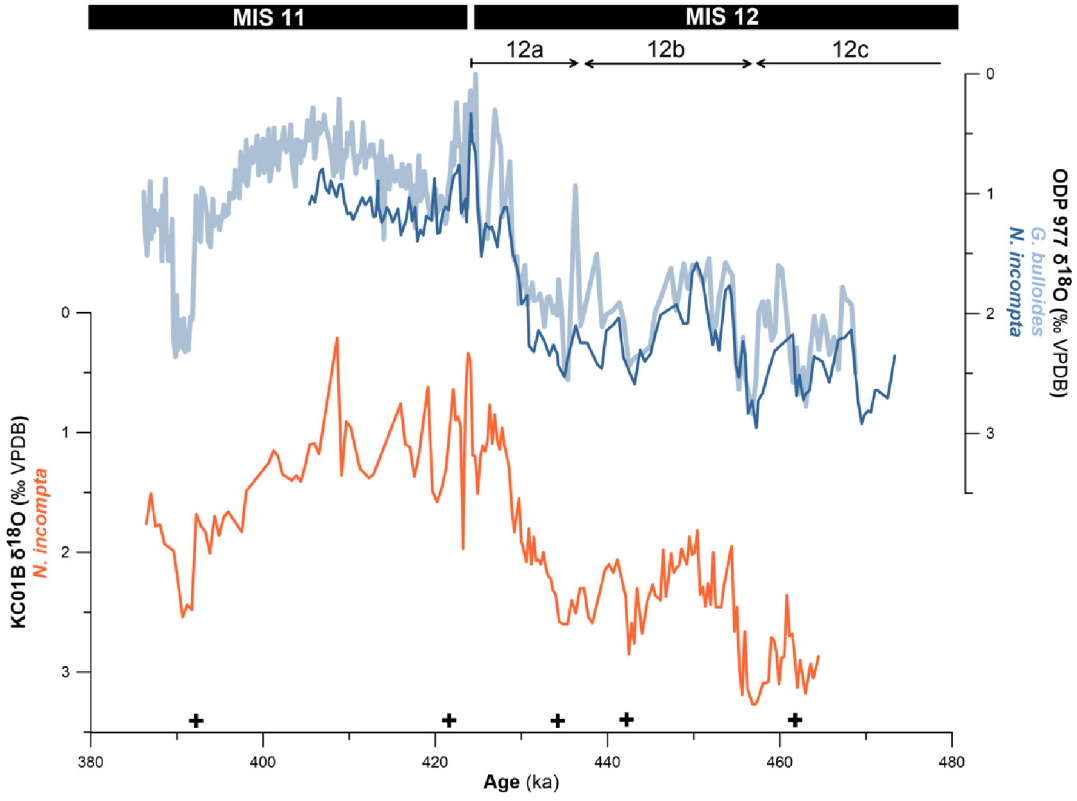

Fig. 3. KC01B age calibration of the studied interval by correlating δ^{18}O measurements in *N. incompta* and *G. bulloides* from ODP Site 977 (dark and light blue) with *N. incompta* δ^{18}O curve from site KC01B (orange) (Capotondi et al., 2016). The crosses over the time axis (ka) are the primary control points established in this study. Substages from Railsback et al. (2015) and MIS 12/MIS 11 boundary from Lisiecki and Raymo (2005). (For interpretation of the references to colour in this figure legend, the reader is referred to the Web version of this article.)

uncertainties of the Pozzolane Rosse tephra chronology described in Lake Ohrid (457 ± 2 ka) (Leicher et al., 2016).

4. Results

The studied interval covers most of MIS 12 and the earlier part of MIS 11. For ODP Site 977, 18 taxonomical categories of planktonic foraminifers were identified in the analysed assemblages including six major species, i.e. *N. incompta* (= *Neogloboquadrina pachyderma* dextral), *Neogloboquadrina pachyderma* (= *Neogloboquadrina pachyderma* sinistral), *G. bulloides*, *Globoconella inflata* (= *Globorotalia inflata*), *Globigerinoides ruber* white, *Globigerinita glutinata*

and *Turborotalita quinqueloba*. Four influxes of the polar species *N. pachyderma* (Bé and Hutson, 1977) were identified from 463 to 425 ka, showing relative abundances up to 25 % (Fig. 4c). For KC01B, 21 taxonomical categories of planktonic foraminifers were recognized. Unlike ODP Site 977, the relative abundance of *N. pachyderma* in KC01B always remained below 2%, although the abundance pattern of the species displays some similarities with that observed at ODP 977 with higher abundances during *N. pachyderma* influxes for the latter (Fig. 4c).

These *N. pachyderma* influxes in the Mediterranean (Girone et al., 2013; Marino et al., 2018) have been associated to extremely low SST and $\delta^{18}O$ drops in the Atlantic (Marino et al., 2014; Palumbo et al., 2013; Rodrigues et al., 2011; Voelker et al., 2010). Some of them were triggered by iceberg melting episodes and have been correlated with the North Atlantic ice-rafted detritus (IRD) rich layers similar to the Heinrich events of the last glacial period (Andrews and Voelker, 2018; de Abreu et al., 2003; Eynaud et al., 2009; Martrat et al., 2007; Naughton et al., 2009). Although IRDs are not detected within the Mediterranean, the intervals with high relative abundances of *N. pachyderma* are clearly related to Heinrich stadials. Due to similarities between the North Atlantic, Iberian Margin and Mediterranean records, and in order to be consistent with other studies (Capotondi et al., 2016; Girone et al., 2013; Marino et al., 2018; Rodrigues et al., 2011), the nomenclature proposed by Rodrigues et al. (2011) for the MD03-2699 record is applied (Ht4 to Ht7).

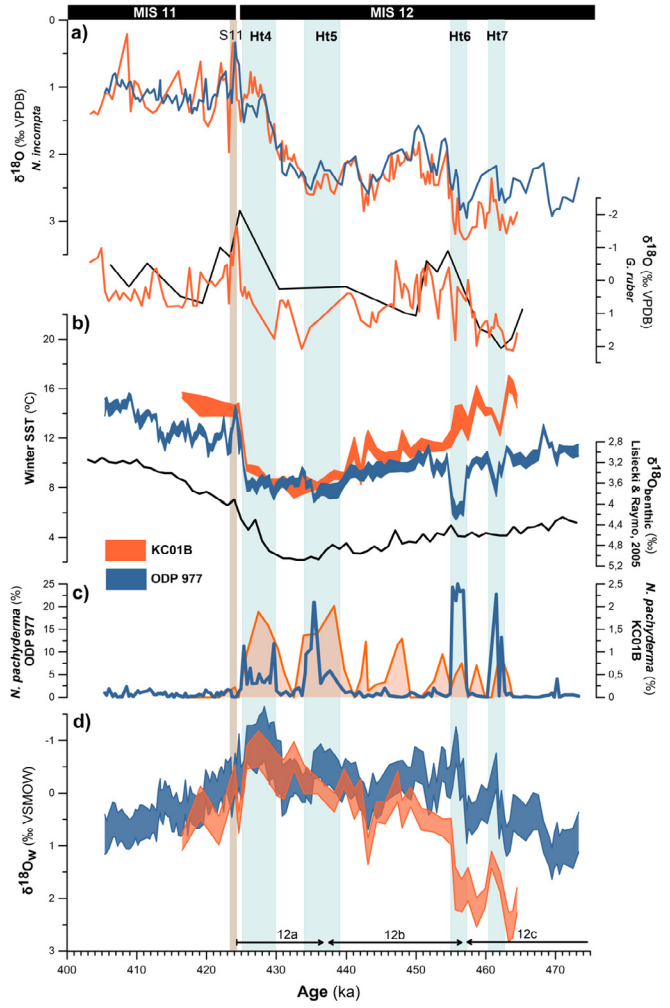

Fig. 4. (a) ODP Site 977 and KC01B *N. incompta* $\delta^{18}O$ records compared with the KC01B $\delta^{18}O$ curves of *G. ruber* from Capotondi et al. (2016) (orange), from Rossignol-Strick and Paterne (1999) (black). (b) Winter mean paleotemperatures of the studied interval reconstructed using the ANN technique and benthic $\delta^{18}O$ global record (black line) from Lisiecki and Raymo (2005). The thickness of the temperature plots reflects the uncertainties in the SST estimates. (c) Relative abundance of *N. pachyderma* and (d) calculated isotopic composition of the surface water ($\delta^{18}O_w$) in ODP 977 and KC01B studied samples. The thickness of the oxygen isotope plots corresponds to the uncertainties in the SST estimates propagated in the $\delta^{18}O_w$ reconstruction. Light blue vertical bars delimitate intervals defined as Heinrich stadials and light brown vertical bar delimitate the time of sapropel S11 deposition in the Ionian Sea (Capotondi et al., 2016). MIS 12 substages from Railsback et al. (2015) and MIS 12/MIS 11 boundary from Lisiecki and Raymo (2005). (For interpretation of the references to colour in this figure legend, the reader is referred to the Web version of this article.)

The sea surface temperature decreased in both records along MIS 12, as described in other North Atlantic and Mediterranean studies (Alonso-Garcia et al., 2011b; Capotondi et al., 2016; Girone et al., 2013; Rodrigues et al., 2011, 2017; Stein et al., 2009). Although the Ionian SSTs during MIS 12c and the onset of MIS 12b were significantly warmer than the Alboran ones (Fig. 4b), lower temperatures as low as 7 °C during the glacial maximum MIS 12a were similar in both regions. This cooling trend was abruptly broken during Termination V with a 5–7 °C warming event recorded at both sites.

The lowest winter temperatures of 5.5 °C were reached in ODP Site 977 during Heinrich stadials, coinciding with the invasions of polar species to the Mediterranean; these SST drops are not so evident at KC01B. During MIS 11 two phases can be differentiated at ODP Site 977, the interval from 424 to 415 ka with mostly constant and lower temperatures and the interval younger than 413 ka characterized by average higher temperatures. Both intervals are separated by a minor cooling event. After 411 ka SST increased reaching the absolute maximum of 16.65 °C on ODP Site 977 until the end of the interval coinciding with the beginning of the late MIS 11c (405–397 ka), a potential Holocene analogue (Berger and Loutre, 2003; Capotondi et al., 2016; de Abreu et al., 2005; Desprat et al., 2005, 2007; Droxler and Farrell, 2000; Kandiano et al., 2012; Loutre, 2003; McManus et al., 2003; Tzedakis, 2010). This thermal trend for early MIS 11 has been described previously in Atlantic records from the Portuguese margin (Voelker et al., 2010). During the studied interval of the MIS 11, the Ionian record exhibits higher winter SST than the Alboran Site.

The *N. incompta* $\delta^{18}O$ records in ODP Site 977 and KC01B follow very similar trends during MIS 12 and 11 (Fig. 4a). The two records show a significant drop in early MIS 12b at around 455 ka and the second one within MIS 12a at ~435 ka.

5. Discussion

Paradoxically, both the Alboran isotope record, reflecting the Atlantic influence, and the Ionian $\delta^{18}O_w$ record with a more Mediterranean isotope imprint, show an opposite behaviour to the global $\delta^{18}O$ LR04 stack (Fig. 4d) and to $\delta^{18}O_w$ changes for glacial periods outside the Mediterranean Sea (Elderfield et al., 2012; Sosdian and Rosenthal, 2009), which display the characteristic high $\delta^{18}O$ values of a prominent glacial period. This is especially anomalous because, in addition to the global effect of the large ice volume during this stage, a Mediterranean $\delta^{18}O$ enrichment of around 2.5‰ is expected due to the effect of the restricted connection with the Atlantic during glacials (Grant et al., 2012). The potential causes of these oxygen isotope anomalies and their possible relationship with Atlantic or Mediterranean freshwater sources will be discussed below.

5.1. Variations in the $\delta^{18}O$ of the atlantic inflow during MIS 12

The decreasing trend and rather low $\delta^{18}O_w$ values recorded during MIS 12 at ODP Site 977 (Fig. 4d) must be the result of

continuous advection of ^{18}O-depleted waters from the Atlantic. The freshwater anomalies observed at ODP Site 977 extend throughout the glacial period, although in this study we analysed the interval from 473 to 424 ka and they were found to be especially pronounced during Heinrich stadials Ht4-Ht7, when the most significant $\delta^{18}O_w$ decreases were observed at ODP Site 977.

The coincidence of this long decrease of $\delta^{18}O$ of surface water at the entrance of the Mediterranean with the decrease in the benthic $\delta^{13}C$ in the Atlantic suggests that both records can be related to a common causal mechanism. We assume that the decrease of Atlantic benthic $\delta^{13}C$ was caused by meltwater release from the ice-sheets that weaken the Atlantic Meridional Overturning Circulation (AMOC). In consequence, the periods with low benthic $\delta^{13}C$ should be linked to high meltwater inputs to the Atlantic and thus decreasing $\delta^{18}O_w$ of the Atlantic inflow. The glacial MIS 12 is characterized by slow north Atlantic thermohaline circulation caused by the release of meltwater from the Eurasian and Laurentide ice-sheets, which is reflected in the low benthic $\delta^{13}C$ all over the Atlantic (Hodell et al., 2008; Toucanne et al., 2009; Voelker et al., 2010) (Fig. 5c). These Atlantic freshwater anomalies caused by meltwater derived from the Eurasian and Laurentide ice-sheets instabilities during MIS 12 reached the Mediterranean when the NE Atlantic surface circulation promoted their propagation to the Strait of Gibraltar. This occurred especially during Heinrich stadials when the polar front and the subtropical gyre shifted southward (Alonso-Garcia et al., 2011a; Barker et al., 2015; Bond and Lotti, 1995; Broecker et al., 1992; Broecker, 1994; Hodell et al., 2017; Peck et al., 2006, 2007). The enhancement of the freshwater fluxes triggered a shutdown of the AMOC, and the southward shift of the polar front favoured the advection of polar and less saline water into the Mediterranean (Palumbo et al., 2013; Rodrigues et al., 2011; Sierro et al., 2020; Sierro et al., 2005; Voelker et al., 2009; Voelker and de Abreu, 2011). Cooler and less salty waters are conveyed to the Mediterranean throughout the Portuguese margin by the Portugal Current, reducing the prevalence of subtropical saltier waters from the Azores Current.

A higher influence of the PC in the western Portuguese margin was reported during late MIS 12b and MIS 12a, especially between 440 and 430 ka (Palumbo et al., 2013; Rodrigues et al., 2011; Voelker et al., 2010). The great amounts of meltwater delivered from the large ice-sheets over North America and northwest Europe during MIS 12 are recorded in the Atlantic by depletions in the planktonic $\delta^{18}O$, sometimes accompanied by IRD deposits (Fig. 5) (Alonso-Garcia et al., 2011b; Hodell et al., 2008; McManus et al., 1999; Naafs et al., 2014; Oppo et al., 1998; Rodrigues et al., 2011; Stein et al., 2009; Toucanne et al., 2009; Voelker et al., 2010). Although the first $\delta^{18}O$ depletion in the Alboran Sea recorded at 468 ka is not related to any Heinrich stadial, we correlated these Heinrich events in the Northeast Atlantic with the freshening events Ht7, Ht6, Ht5 and the most prominent in Ht4 during the Termination, between 463 and 425 ka (Fig. 5) (Girone et al., 2013; Maiorano et al., 2016; Marino et al., 2018; Rodrigues et al., 2011). These $\delta^{18}O_w$ drops are accompanied by sea surface water cooling in the Alboran Sea and invasions of the polar species *N. pachyderma* (Figs. 4 and 5). These events of high abundance of *N. pachyderma* and surface cooling have also been recorded in the Balearic and Ionian seas, associated with low $\delta^{18}O$ planktonic foraminifer values (Capotondi et al., 2016; Girone et al., 2013) (Fig. 5).

Although the dolomitic composition of IRDs from Site U1313 is characteristic of Laurentide ice-sheet origin, the meltwaters and icebergs captured by the PC could correspond both with either Laurentide and/or Fennoscandian ice-sheets. Indeed, the highest terrigenous accumulation rates of the last 1.2 Ma were reported in the Bay of Biscay between 468 and 425 ka (Fig. 5), with rather high Ti/Ca ratios as well (Toucanne et al., 2009). Those events were linked to huge meltwater discharges from the Fennoscandian ice-sheet, supporting the instability of these continental ice masses during MIS 12. The most prominent discharge, which occurred between 461 and 456 ka, has been associated with the opening of the Dover Strait and the catastrophic drainage of previous proglacial lakes (Hodell et al., 2019; Toucanne et al., 2009).

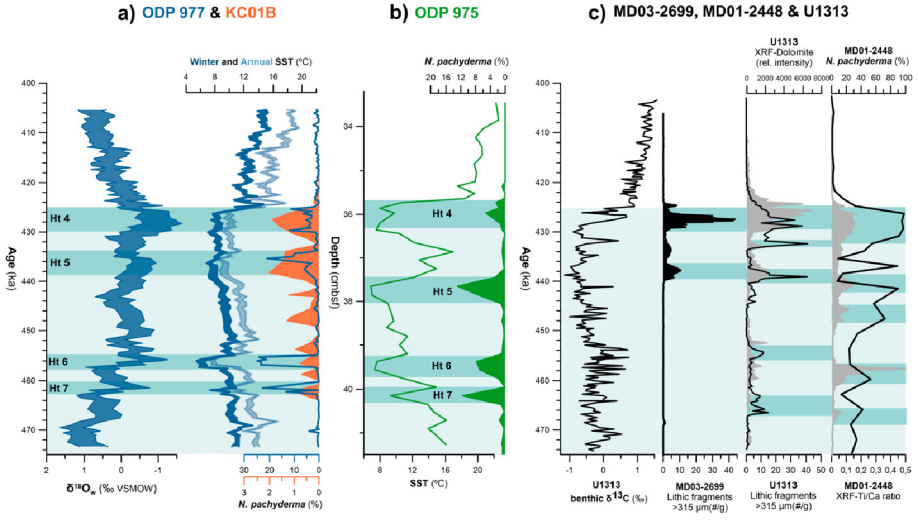

Fig. 5. a) Oxygen isotopic composition of the surface water and winter (dark blue) and annual (light blue) SST records for ODP Site 977, *N. pachyderma* relative abundances in ODP Site 977 and KC01B compared to (b) SST curve and *N. pachyderma* distribution pattern at ODP Site 975 (Girone et al., 2013). (c) $\delta^{13}C$ record of the benthic foraminifera *Cibicidoides wuellerstorfi* from U1313 (Voelker et al., 2010). Lithic fragments content in MD03-2699, lithic fragments (black line) and Dolomite (filled grey) composition detected by XRF analysis (Stein et al., 2009) and Ti/Ca XRF-derived ratio (filled grey line) and *N. pachyderma* relative abundances (black line) in samples of core MD01-2448 (Toucanne et al., 2009). Lighter blue interval marks glacial MIS 12 and darker blue bars the Heinrich stadials in the Mediterranean and Heinrich events in the Atlantic. (For interpretation of the references to colour in this figure legend, the reader is referred to the Web version of this article.)

5.2. Impact of the mediterranean hydrology on the oxygen isotope gradient between Alboran and Ionian seas during MIS 12

In the Ionian Sea, a similar decreasing trend of the $\delta^{18}O_w$ is observed along most of MIS 12 (Fig. 6a), but now these values reflect the $\delta^{18}O_w$ signature carried from the Atlantic and its modifications along the course of the MAW from the Alboran to the Ionian. This oxygen isotope modification is caused by the Mediterranean hydrologic budget and water exchange with the Atlantic (Rohling, 1999). In order to evaluate the impact of the Mediterranean hydrologic budget on the $\delta^{18}O$ signature of the MAW along its flow to the eastern Mediterranean, we calculated the longitudinal $\delta^{18}O_w$ Mediterranean gradient during MIS 12 (Fig. 6b), which ranges between 2.78‰ and −0.76‰.

Along MIS 12, we observed two periods with distinctly different $\delta^{18}O_w$ gradients between the western and eastern Mediterranean (Fig. 6b). (1) The highest seawater $\delta^{18}O$ gradients are recorded during MIS 12c and the onset of MIS 12b before 455 ka. (2) After 455 ka (MIS 12b and 12a), the inter-basin differences are reduced until the beginning of the MIS 11 at 424 ka. This change in the Mediterranean hydrologic budget occurred briefly after the deposition of the Pozzolane Rosse tephra, dated at 457 ± 2 ka (Leicher et al., 2016) (MIS 12b/12b boundary), which correlates in time with the tephra I24 identified in core KC01B (Lourens, 2004) (ca. 458 ka in this study).

Toward the glacial maximum, the Mediterranean $\delta^{18}O_w$ gradient remained below current values and reached negative values during a significative interval between Ht5 and Ht4 (Fig. 6b). These extremely low oxygen isotope gradients, especially during the glacial maximum (late MIS 12b and MIS 12a), are even more anomalous if we consider the great amplitude of the sea level drop recorded during that time (Fig. 6c) and its estimated impact on the Mediterranean surface $\delta^{18}O_w$ due to the reduced Atlantic Mediterranean water exchange (Rohling et al., 2014). The reduced water

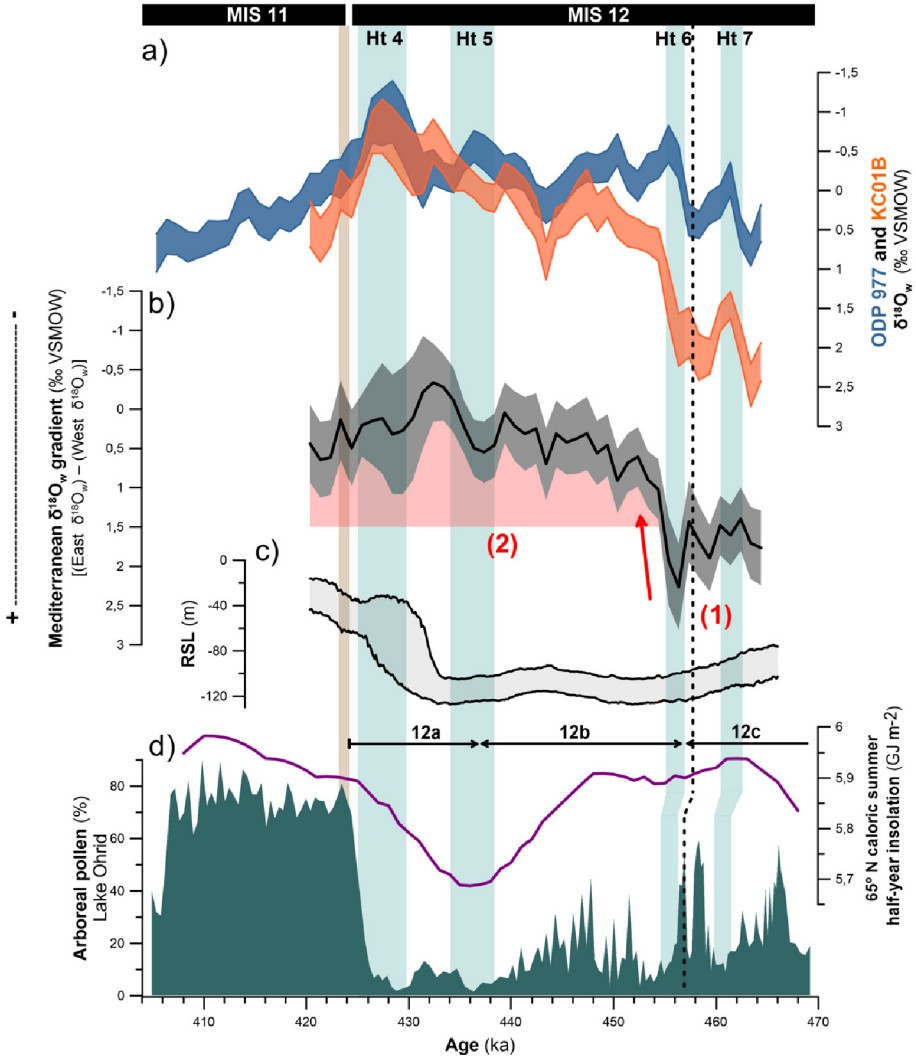

Fig. 6. a) Reconstructed oxygen isotopic composition of the sea surface waters in both ODP 977 and KC01B sites for MIS 12 and the deglaciation and (b) calculated longitudinal Mediterranean $\delta^{18}O_w$ gradient. The thickness of the plots corresponds to the uncertainties in the $\delta^{18}O_w$ reconstruction, (1) Interval before 455 ka with highest $\delta^{18}O_w$ gradients and (2) after 455 ka with lower $\delta^{18}O_w$ gradients. c) Relative sea level (RSL) record from Grant et al. (2014). d) Arboreal pollen (%) record from the Lake Ohrid (Koutsodendris et al., 2019) and 65° N caloric summer half-year insolation from Tzedakis et al. (2017). Light blue vertical bars delimitate intervals defined as Heinrich stadials and light brown vertical bar delimitate the time of sapropel S11 deposition in the Ionian Sea (Capotondi et al., 2016). Ht7 and Ht6 were correlated with LO-12-8c and 6c events in Lake Ohrid according to Koutsodendris et al. (2019). The dashed vertical line indicates the Pozzolane Rosse tephra (457 ± 2 ka) in Lake Ohrid (Leicher et al., 2016) and the presumably equivalent tephra I24 in KC01B (ca. 458 ka in this study) (Lourens, 2004). Substages from Railsback et al. (2015) and MIS 12/MIS 11 boundary from Lisiecki and Raymo (2005). (For interpretation of the references to colour in this figure legend, the reader is referred to the Web version of this article.)

exchange with the Atlantic should have increased the residence time of the water inside the Mediterranean, and its exposure to a negative hydrologic budget for a longer time should have increased the $\delta^{18}O_w$ between the Alboran and Ionian seas. Nevertheless, very low longitudinal Mediterranean gradient values are observed when a maximum gradient was expected.

The higher seawater $\delta^{18}O$ gradients recorded before 455 ka are probably the result of reduced freshwater inputs to the Mediterranean or a heavier $\delta^{18}O$ freshwater flux. This high $\delta^{18}O_w$ gradient can be expected for a glacial period with typically negative water budgets and low rates of water exchange with the Ocean. However, the low gradients after 455 ka are totally unexpected, considering the low water exchange with the Atlantic and the dry and cold conditions. In addition to the restriction in the water exchange between the Mediterranean and the Atlantic, the sea level lowstand should have also reduced the effective exchange area between the two Mediterranean basins through the Strait of Sicily, further increasing the residence time of the water in the eastern basin, and thus increasing the longitudinal isotopic gradient (Grant et al., 2016; Rohling et al., 2014; Rohling, 1999).

MIS 12 is a severe glacial period and is considered one of the driest and coldest periods of the Pleistocene over the Mediterranean area as evidenced by a constant reduction trend in tree population with the absolute minimum extension, and higher steppic taxa presence, during early MIS 12b and MIS 12a between 440 and 426 ka (Fig. 6d) (Koutsodendris et al., 2019; Pross et al., 2015; Sadori et al., 2016; Tzedakis et al., 2006). These conditions should have increased the negative water budget of the Mediterranean Sea. Only a lower $\delta^{18}O$ of the precipitation linked to the lower $\delta^{18}O$ of the Atlantic source of the moisture advected to the Mediterranean could explain the lower $\delta^{18}O_w$ gradient, as reported for other periods (Bar-Matthews et al., 2003; Domínguez-Villar et al., 2009). Although the lower $\delta^{18}O$ of the precipitation would be expected during Heinrich stadials when the Atlantic surface water reached the lowest $\delta^{18}O$, higher longitudinal $\delta^{18}O_w$ Mediterranean gradients are found during these intervals.

Therefore, the offset between the expected high $\delta^{18}O_w$ gradient and the low gradient observed in this study after 455 ka, and especially the negative gradients toward the glacial maximum, must have been triggered by a greater flux of freshwater into the Mediterranean, which is not related to enhanced annual rainfall or to a decrease of the $\delta^{18}O$ of the precipitation in the Mediterranean region. Although major freshwater anomalies are propagated from the Atlantic, as explained above, the larger oxygen isotope depletions seen in the Ionian Sea compared to Alboran can only be explained by additional freshwater inputs to the Ionian Sea and potentially to the eastern basin in general. Similar eastern Mediterranean freshwater anomalies can be foreseen for MIS 14 and MIS 16 when important oxygen isotope depletions have been also identified in the eastern Mediterranean $\delta^{18}O$ stack (Lourens, 2004; Rohling et al., 2014; Wang et al., 2010). As a consequence, we can conclude that, at least after 455 ka, a great volume of freshwater (or water with lower $\delta^{18}O$) flowed into the Mediterranean and contributed to lower the $\delta^{18}O_w$ in addition to the freshwater that entered from the Atlantic through the Strait of Gibraltar. In section 5.3, the potential sources of this freshwater will be further explored.

Although seawater $\delta^{18}O_w$ and salinity are water budget dependent, changes in both properties are not linear because the $\delta^{18}O_w$ is a function of the volumes and oxygen isotope imprints of the evaporated water and freshwater inputs to the Mediterranean. Therefore, a negative Mediterranean $\delta^{18}O_w$ gradient does not necessarily have to be linked to a salinity gradient inversion, although it corresponds to a reduction in the absolute value.

5.2.1. Higher longitudinal mediterranean seawater $\delta^{18}O$ gradients during heinrich stadials

Superimposed to the previously described general trend before and after 455 ka, we identified a series of intervals with distinct relative higher $\delta^{18}O_w$ gradient values that correspond to the defined Heinrich stadials. In particular, remarkable increases in the longitudinal Mediterranean $\delta^{18}O_w$ gradient values are recorded during Ht6 and Ht5 that register $\delta^{18}O$ depletions in both eastern and western records, but the negative anomalies at ODP Site 977 exceed those observed in KC01B (Fig. 6a). These data undoubtedly reflect the propagation of ^{18}O-depleted water from the Atlantic inflow, probably due to a higher influence of the PC at the Strait of Gibraltar during these Heinrich stadials (Palumbo et al., 2013; Rodrigues et al., 2011; Sierro et al., 2005, 2020; Voelker et al., 2010). Although meltwater input to the eastern basin has been observed during Heinrich stadials (Martinez-Lamas et al., 2020), the Atlantic inflow $\delta^{18}O_w$ anomalies are relatively larger. This $\delta^{18}O_w$ decrease is mitigated to the east as observed in the higher $\delta^{18}O_w$ gradient probably as a consequence of more extreme negative Mediterranean hydrologic budget during these events. This is consistent with the extremely arid conditions documented during Heinrich stadials in the Mediterranean region (Cacho et al., 2000; Goñi et al., 2002). In a high-resolution palynological study of Lake Ohrid for MIS 12, Ht7 (contraction event LO-12-6c), Ht6 (contraction event LO-12-8c), Ht5 and Ht4 are synchronous to forest extension minima (Fig. 6d) and steppic taxa maxima, which characterized coldest and driest conditions (Koutsodendris et al., 2019). Similar evidences have been observed in the Sulmona basin lacustrine record where lake level drops, triggered by precipitation minima, were identified during these Heinrich stadials, especially during Ht6, Ht5 and Ht4 (Regattieri et al., 2016). These arid conditions would modify the ^{18}O-depleted incoming water at the entrance of Gibraltar into an ^{18}O-enriched water along its transit from the Alboran to the Ionian Sea and explain the relative higher longitudinal Mediterranean gradients during the Heinrich stadials.

5.3. Potential freshwater sources in the eastern mediterranean

5.3.1. African monsoon

One of the main freshwater sources to the eastern Mediterranean, principally during sapropel formation, is the Nile river discharge due to maximum intensity of the African monsoons triggered by northern Hemisphere summer insolation maxima (Bethoux, 1993; Grant et al., 2016; Jenkins and Williams, 1984; Rohling, 1994; Rossignol-Strick et al., 1982). Two periods of stronger Asian monsoons were recorded during the MIS 12, associated to low amplitude summer insolation maxima at 465 and 446 ka (Cheng et al., 2016). Assuming that changes in the intensity of Asian and African monsoons were synchronous, high Nile discharge to the Mediterranean Sea would be anticipated. However, no sapropel has been identified in the eastern Mediterranean during MIS 12 (Konijnendijk et al., 2014). The absence of sapropels (Lourens et al., 1996; Wehausen and Brumsack, 2000) suggests low Nile discharge into the eastern basin. Furthermore, the decrease in $\delta^{18}O_w$ at 455 ka in the eastern Mediterranean, and especially the extreme low $\delta^{18}O_w$ recorded at the end of MIS 12, cannot be linked to the African monsoons since they were extremely weak during that time (Cheng et al., 2016). As a consequence, a different freshwater source is needed to explain these low and negative $\delta^{18}O_w$ longitudinal Mediterranean gradients during MIS 12.

5.3.2. Black Sea inflow

During the last glacial period, and especially during Heinrich stadials, there is strong evidence of freshwater discharge from the Fennoscandian and north-east Alpine ice-sheets to the Caspian and

Black seas through the Dnieper, Dniester, Volga and Danube rivers, and potentially to the eastern Mediterranean (Bahr et al., 2005, 2006, 2008; Major et al., 2002, 2006; Martinez-Lamas et al., 2020; Ryan et al., 2003; Soulet et al., 2010). Additionally, synchronous Alpine drainage events to the Black and Adriatic seas have been reported for the Heinrich stadials during the last glacial period (Martinez-Lamas et al., 2020; Rossato and Mozzi, 2016), suggesting additional freshwater sources to those observed at Gibraltar.

As reported for the last glacial period, during MIS 12 the Black Sea would have been a giant brackish 'lake' isolated from the Marmara and Mediterranean seas, and its hydrologic budget would have been mainly driven by the evolution of the southern margin of the Fennoscandian ice-sheet and its meltwater draining episodes. Although there is little information about MIS 12, input of ^{18}O-depleted meltwaters to the Black Sea during the last glaciation has been related to red clay layers (Bahr et al., 2005, 2008; Major et al., 2002, 2006; Mangerud et al., 2004; Tudryn et al., 2016) which, in turn, have been linked to the retreat of the Scandinavian ice-sheet between 17.2 and 15.7 ka (Soulet et al., 2013). Studies in the Marmara Sea suggest that this meltwater could have overflowed the Dardanelles Strait and thus reach the Mediterranean (Aloisi et al., 2015; Soulet et al., 2010, 2013; Vidal et al., 2010). During MIS 12, when the Eurasian ice-sheet reached its maximum extension, the freshwater input to the Black Sea and possibly to the Mediterranean could have been even larger. The retreat of the southern margin of the eastern Fennoscandian ice-sheet probably resulted in the formation of proglacial lakes that eventually drained to the Caspian or Black seas, as occurred during the last glacial maximum. Studies of north Germany glaciation evidenced a major continental glaciation during MIS 12 with large ice-sheets advances and evidences of eastern meltwater drainage to the Danube and the Black Sea (Ehlers et al., 2011 and references therein).

The impact of meltwater drained from the southern margin of the Fennoscandian ice-sheet would have had a high impact on the Mediterranean $\delta^{18}O_w$ because of its very negative oxygen isotope values. For MIS 12, when comparing the *G. ruber* δ^{18}O record from ODP Site 967 in the eastern Mediterranean with the *G. ruber* δ^{18}O from KC01B in the Ionian Sea (Capotondi et al., 2016; Wang et al., 2010), the most significant oxygen isotope depletions are found in the Ionian Sea. Due to the predominant anti-clockwise circulation of the Levantine basin (Fig. 1a), the salinity and $\delta^{18}O_w$ decrease caused by a freshwater input from the Black Sea would firstly influence the surface water at core KC01B location rather than that of ODP Site 967.

5.3.3. Drainage to the Adriatic Sea

Another potential source of freshwater, which could have contributed to the isotope depletion of the Mediterranean surface water during MIS 12, was the drainage of the southern Alpine, Apennines and Balkan ice-sheets into the Adriatic basin. It is worth noting that the eastern sector of the Adriatic Sea is surrounded by the Dinaric and the Pindus mountain range that cover large part of the eastern Europe area. Existing data document that during some Pleistocene glaciations these mountains hosted glacial valleys and cirques that would have drained though river systems into the Adriatic Sea, and thus potentially into the Ionian Sea propagating the ^{18}O-depleted water to the location of core KC01B. In detail, for the largest recorded glaciation dated >350 ka and correlated to MIS 12, moraines at altitudes below 1000 m were identified (Adamson et al., 2014, 2017; Hughes et al., 2007, 2010, 2011; Leontaritis et al., 2020; Marjanac and Marjanac, 2016; Woodward et al., 2008). Although these glaciers were numerous, they accumulated much lower ice volume than the Alpine of the Fennoscandian ice-sheets. While glaciers up to 165 km^2 and ca. 450 m thick have been described for this period in Montenegro (Hughes et al., 2010), the Alpine ice-sheet has been estimated to be ~130,000 km^2 for the last glacial maximum, with ~50,000 km^2 drained into the Black Sea and the rest to the Adriatic Sea though the Po river (Ehlers and Gibbard, 2004; Martinez-Lamas et al., 2020). Therefore, although there must have been a contribution from the Balkans and Apennines ice caps, due to the considerable size difference, the Alpine ice-sheet should have been the main freshwater input to the Adriatic Sea.

The study of the Brenta south-alpine glacier, which drained into the Adriatic via the Po river during the last glacial maximum, revealed a sequence of regressions and glacier advances synchronous with fluctuations in the discharge regime of the Danube river into the Black Sea (Rossato and Mozzi, 2016). Evidence of Danube flood activity during the last glacial maximum was highly correlated with Po river drainage activity (Martinez-Lamas et al., 2020); north-east and south-east Alpine glacier deglaciation and draining were synchronous. Recent studies also suggest extensive Mediterranean glacier retreat during the Heinrich stadials of the last glacial period (Allard et al., 2021). The volume of ice stored in the Alps during MIS 12 was probably larger than that recorded in other glacial periods, and thereby the freshwater contribution to the Mediterranean, when these ice masses became unstable, should also have been higher. This means that ice accumulation in the Alps during MIS 12 was very high, and the instabilities of these ice-sheets, probably driven by increases in the summer energy (Huybers, 2006), generated large amounts of meltwater that left an important isotope imprint in the $\delta^{18}O_w$ of the eastern Mediterranean. From 465 to 445 ka, high values of the caloric summer half-year, which is almost equivalent to the summer energy (Fig. 6c), were related by Tzedakis et al. (2017) to incomplete deglaciations, which would have triggered higher melting rates in the very dynamic Alpine glacier (Seguinot et al., 2018).

Core KC01B could have been strongly affected by freshwater discharge from the Po because of the southern shift of the coastline from 44.5°N to 41.5°N during the lowstand of MIS 12. The marine regression and the subsequent fluvial erosion towards the south increased the flow and drainage area, as reported for the last glacial period (Amorosi et al., 2016; Ivy-Ochs et al., 2006; Maselli et al., 2014; Monegato et al., 2007; Ravazzi et al., 2014), and a larger freshwater discharge would have had a larger impact on the Ionian Sea and surface water at KC01B. Furthermore, the highly negative δ^{18}O signature of the meltwater derived from the Alps would have had a greater impact on the Mediterranean $\delta^{18}O_w$ decrease.

5.4. Freshwater input during Ht4 and eastern mediterranean stratification preceding sapropel S11

The extremely low $\delta^{18}O_w$ during Termination V, coinciding with Ht4 in the Alboran and Ionian seas, is the result of the entrance of a large flow of freshwater from Gibraltar and from the Alpine ice-sheet through the Po river and/or through the Black Sea. This freshwater anomaly, largely amplified by the sea level rise and the deepening and widening of the Gibraltar and Sicily straits (Grant et al., 2016; Matthiesen and Haines, 2003; Rohling et al., 2014, 2015), spread along the surface, decreased sea surface salinity and increased the vertical density gradient in the Mediterranean. This has been clearly recorded by the formation of a DCM at site KC01B, as was inferred in Capotondi et al. (2016) from the high abundance of *N. incompta* and *N. dutertrei* during this time period. The formation of a DCM is characteristic of many sapropels due to the concentration of nutrients near the pycnocline when a strong density gradient is developed between the low-density surface and high-density subsurface waters (e.g. Emeis and Party, 1996; Grimm et al., 2015; Rohling, 1994; Rossignol-Strick et al., 1982). The stratification during Ht4 is also inferred from the high Ba/Al ratio (Langereis et al., 1997) and the low colour reflectance that preceded

and continued during the formation of sapropel S11 (Figs. 4 and 6), not only in core KC01B (Lourens, 2004) but also in ODP Sites 967 and 968 (Konijnendijk et al., 2014). It also coincides with a low Ti/Al ratio that is normally tuned to summer insolation maximum, as is the case for this DCM-sapropel S11 episodes (428 ka insolation maximum, i-cycle 40) (Konijnendijk et al., 2014).

Consequently, we conclude that the freshwater entry to the Mediterranean during Termination V was the first step towards the buoyancy gain of Mediterranean surface water, increasing the stratification of the water column and thus promoting the preconditioning for sapropel formation (Rohling et al., 2015), that decreased deep water ventilation, thus increasing organic matter preservation in the seafloor. However, complete bottom water stagnation in the eastern Mediterranean and formation of sapropel S11 only happened at the end of Termination, which is registered both in the Alboran and Ionian seas. This indicates that full anoxic conditions during S11 were only reached a few ka after the initial preconditioning as suggested for S1 (Grimm et al., 2015). It seems that (Figs. 4 and 6) full bottom anoxia at the base of S11 was triggered by the surface water warming recorded at that time probably triggered by decreased heat loss to the atmosphere due to the warmer winter air reaching the northern Mediterranean after the AMOC resumption during Termination V, as has been proposed for more recent sapropels (Sierro et al., 2020).

Other freshwater inflows that could be responsible for the Mediterranean preconditioning for stratification are the African monsoons and Mediterranean annual rainfall. Intensification of African monsoon, which has been traditionally behind the formation of Mediterranean sapropels, was relatively weak at that time (Cheng et al., 2016) and probably only played a minor role in water stratification. In contrast, a rainfall increase at the beginning of MIS 11 was recorded in palynological records (Fig. 6d) (Koutsodendris et al., 2019) and thus could have further contributed to Mediterranean stratification.

6. Conclusions

Comparison of the oxygen isotope surface water records from core ODP 977 and KC01B, collected in the Alboran and Ionian seas, respectively, allowed us to reconstruct changes in the $\delta^{18}O_w$ of the Atlantic inflow and the impact of the Mediterranean hydrology on the $\delta^{18}O$ of Mediterranean water during MIS 12.

An increase of Mediterranean surface $\delta^{18}O_w$ was expected during MIS 12 because of the high net freshwater loss and the longer residence time of the water in the Mediterranean, due to the lower Atlantic-Mediterranean and western-eastern basins water exchanges during the glacial lowstand. In contrast, lower $\delta^{18}O_w$ values than today have been observed both in the Alboran and Ionian seas, especially between 455 ka and the end of MIS 12 (424 ka). A large fraction of the freshening, characterized by low $\delta^{18}O_w$ values, lowest temperatures and high abundances of *N. pachyderma*, entered the Mediterranean through the Atlantic inflow, especially during Heinrich stadials, due to the southward migration of the polar front and the prevalence of the Portugal Current in the Atlantic inflow to the Mediterranean.

However, data of the Mediterranean $\delta^{18}O_w$ gradient allowed us to identify other sources of freshwater to the Mediterranean basins. From 455 ka to the end of MIS 12 (424 ka), the $\delta^{18}O_w$ gradient was around and below current values, and the gradient became negative during part of the glacial maximum. This negative gradient can only be explained by a significant source of an ^{18}O-depleted freshwater source into the eastern Mediterranean. Based on the proximity of core KC01B to the Adriatic Sea, we speculate that this meltwater source may have been delivered from the Alpine ice-sheet and transported through the Po river to the Mediterranean Sea, even if an important source of meltwater from the Fenno-scandian ice-sheet via the Caspian and Black Sea cannot be ruled out. This evidence resembles the observed influence of the south-east Alpine ice-sheet meltwater drainage into the Adriatic during North Atlantic Heinrich stadials. Therefore, the ice accumulation in the Alps during MIS 12 and meltwater delivery through the Po was large enough to leave an isotope imprint on the eastern Mediterranean $\delta^{18}O_w$. The negative Mediterranean $\delta^{18}O_w$ gradient generated by inter-basin differences in freshwater input does not imply negative salinity gradients. Nevertheless, we can infer lower salinity gradients during MIS 12 between the Alboran and Ionian seas.

The freshwater entry to the Mediterranean amplified by the sea level rise during Termination V, was the first step towards an eastern Mediterranean stratification that decreased deep water ventilation. The complete bottom water stagnation and full bottom anoxia that culminates in the formation of sapropel S11 was only reached at the onset of MIS11 probably triggered by the temperature rise, due to the abrupt warming after the deglaciation, and the increase in rainfall.

Data statement

All data used in this study are available in the Mendeley Data ® public repository as: Azibeiro, Lucia A.; Capotondi, Lucilla; Lirer, Fabrizio; Andersen, Nils; González-Lanchas, Alba; Alonso-García, Montserrat; Flores, José-Abel; Cortina, Aleix; Grimalt, Joan O.; Martrat, Belen; Cacho, Isabel; Sierro, Francisco J. (2021), "Meltwater flux from northern ice-sheets to the Mediterranean during MIS 12 (Data)", Mendeley Data, https://doi.org/10.17632/zjthbx5b7t.2.

Author contribution

Lucía A. Azibeiro: Writing – original draft, Visualization, Project administration. Francisco J. Sierro: Resources, Conceptualization, Supervision, Project administration, Funding acquisition. Lucilla Capotondi: Resources. Fabrizio Lirer: Resources. Nils Andersen: Resources, Formal analysis. Alba González-Lanchas: Resources. Montserrat Alonso-García: Conceptualization. José-Abel Flores: Conceptualization, Supervision, Funding acquisition. Aleix Cortina: Resources. Joan O. Grimalt: Resources. Belen Martrat: Resources. Isabel Cacho: Resources. All authors: prepublication stages review.

Declaration of competing interest

The authors declare that they have no known competing financial interests or personal relationships that could have appeared to influence the work reported in this paper.

Acknowledgments

This work was funded by the FPU contract of the Ministry of Education and Professional Formation FPU2015/03283 awarded to Lucia A. Azibeiro and project RTI 2018-099489-B-100 of the Ministry of Science, innovation and Universities of the Spain government granted to the Grupo de Geociencias Oceánicas (GGO) of the University of Salamanca. The Spanish Ministry of Science and Innovation, Severo Ochoa Project CEX2018-000794-S is likewise acknowledged. We are very grateful to IODP for providing the samples used in this study and appreciate the work of Jose Ignacio Martin Cruz in the picking of planktonic foraminifers for isotope analyses and Marta Casado, Yolanda Gonzalez-Quinteiro, Bibiano Hortelano, Walter Hale and Inma Fernandez for laboratory assistance. We thank the scientific data provided by Samuel Toucanne. The authors thank Philip Hughes and other anonymous reviewer

for their constructive comments and suggestions.

References

Adamson, K., Woodward, J., Hughes, P., 2014. Glaciers and rivers: pleistocene uncoupling in a Mediterranean mountain karst. Quat. Sci. Rev. 94, 28–43. https://doi.org/10.1016/j.quascirev.2014.04.016.

Adamson, K., Woodward, J., Hughes, P., Giglio, F., Del Bianco, F., 2017. Middle Pleistocene glaciation, alluvial fan development and sea-level changes in the Bay of Kotor, Montenegro. Geological Society, London, Special Publications 433, 193–209. https://doi.org/10.1144/SP433.13.

Allard, J.L., Hughes, P.D., Woodward, J.C., 2021. Heinrich Stadial aridity forced Mediterranean-wide glacier retreat in the last cold stage. Nat. Geosci. 1–9. https://doi.org/10.1038/s41561-021-00703-6.

Aloisi, G., Soulet, G., Henry, P., Wallmann, K., Sauvestre, R., Vallet-Coulomb, C., Lécuyer, C., Bard, E., 2015. Freshening of the Marmara Sea prior to its post-glacial reconnection to the Mediterranean sea. Earth Planet Sci. Lett. 413, 176–185. https://doi.org/10.1016/j.epsl.2014.12.052.

Alonso-Garcia, M., Sierro, F.J., Flores, J.A., 2011a. Arctic front shifts in the subpolar North Atlantic during the Mid-Pleistocene (800–400 ka) and their implications for ocean circulation. Palaeogeogr. Palaeoclimatol. Palaeoecol. 311, 268–280. https://doi.org/10.1016/j.palaeo.2011.09.004.

Alonso-Garcia, M., Sierro, F.J., Kucera, M., Flores, J.A., Cacho, I., Andersen, N., 2011b. Ocean circulation, ice sheet growth and interhemispheric coupling of millennial climate variability during the mid-Pleistocene (ca 800-400ka). Quat. Sci. Rev. 30, 3234–3247. https://doi.org/10.1016/j.quascirev.2011.08.005.

Amorosi, A., Maselli, V., Trincardi, F., 2016. Onshore to offshore anatomy of a late Quaternary source-to-sink system (Po Plain–Adriatic Sea, Italy). Earth Sci. Rev. 153, 212–237.

Andrews, J.T., Voelker, A.H.L., 2018. "Heinrich events" (& sediments): a history of terminology and recommendations for future usage. Quat. Sci. Rev. 187, 31–40. https://doi.org/10.1016/j.quascirev.2018.03.017.

Artale, V., Calmanti, S., Malanotte-Rizzoli, P., Pisacane, G., Rupolo, V., Tsimplis, M., 2006. Chapter 5 the Atlantic and Mediterranean Sea as Connected Systems, Developments in Earth and Environmental Sciences, pp. 283–323. https://doi.org/10.1016/S1571-9197(06)80008-X.

Bahr, A., Arz, H.W., Lamy, F., Wefer, G., 2006. Late glacial to Holocene paleoenvironmental evolution of the Black Sea, reconstructed with stable oxygen isotope records obtained on ostracod shells. Earth Planet Sci. Lett. 241, 863–875. https://doi.org/10.1016/j.epsl.2005.10.036.

Bahr, A., Lamy, F., Arz, H., Kuhlmann, H., Wefer, G., 2005. Late glacial to Holocene climate and sedimentation history in the NW Black Sea. Mar. Geol. 214, 309–322. https://doi.org/10.1016/j.margeo.2004.11.013.

Bahr, A., Lamy, F., Arz, H.W., Major, C., Kwiecien, O., Wefer, G., 2008. Abrupt changes of temperature and water chemistry in the late Pleistocene and early Holocene Black Sea. G-cubed 9.

Bar-Matthews, M., Ayalon, A., Gilmour, M., Matthews, A., Hawkesworth, C.J., 2003. Sea–land oxygen isotopic relationships from planktonic foraminifera and speleothems in the Eastern Mediterranean region and their implication for paleorainfall during interglacial intervals. Geochem. Cosmochim. Acta 67, 3181–3199. https://doi.org/10.1016/S0016-7037(02)01031-1.

Barker, S., Chen, J., Gong, X., Jonkers, L., Knorr, G., Thornalley, D., 2015. Icebergs not the trigger for North Atlantic cold events. Nature 520, 333–336. https://doi.org/10.1038/nature14330.

Batchelor, C.L., Margold, M., Krapp, M., Murton, D.K., Dalton, A.S., Gibbard, P.L., Stokes, C.R., Murton, J.B., Manica, A., 2019. The configuration of Northern Hemisphere ice sheets through the Quaternary. Nat. Commun. 10, 1–10. https://doi.org/10.1038/s41467-019-11601-2.

Bauch, H.A., Erlenkeuser, H., 2003. Interpreting Glacial-Interglacial Changes in Ice Volume and Climate from Subarctic Deep Water Foraminiferal δ18O. AGU (American Geophysical Union. https://doi.org/10.1029/137GM07.

Bé, A.W., Hutson, W.H.J.M., 1977. Ecology of Planktonic Foraminifera and Biogeographic Patterns of Life and Fossil Assemblages in the Indian Ocean, pp. 369–414.

Berger, A., Loutre, M.F., 2003. Climate 400,000 years ago, a key to the future? Geophys. Monogr. 17–26. https://doi.org/10.1029/137GM02.

Bethoux, J., 1979. Budgets of the Mediterranean sea. Their dependence on local climate and on the characteristics of Atlantic waters. Oceanol. Acta 9, 59–67.

Bethoux, J.-P., 1993. Mediterranean sapropel formation, dynamic and climatic viewpoints. Oceanol. Acta 16, 127–133.

Bond, G., Broecker, W., Johnsen, S., McManus, J., Labeyrie, L., Jouzel, J., Bonani, G., 1993. Correlations between climate records from North Atlantic sediments and Greenland ice. Nature 365, 143–147. https://doi.org/10.1038/365143a0.

Bond, G., Heinrich, H., Broecker, W., Labeyrie, L., McManus, J., Andrews, J., Huon, S., Jantschik, R., Clasen, S., Simet, C., 1992. Evidence for massive discharges of icebergs into the North Atlantic ocean during the last glacial period. Nature 360, 245–249. https://doi.org/10.1038/360245a0.

Bond, G.C., Lotti, R., 1995. Iceberg discharges into the North Atlantic on millennial time scales during the last glaciation. Science 267, 1005–1010. https://doi.org/10.1126/science.267.5200.1005.

Bond, G.C., Showers, W., Elliot, M., Evans, M., Lotti, R., Hajdas, I., Bonani, G., Johnson, S., 1999. the North atlantic's 1-2 kyr climate rhythm: relation to heinrich events, dansgaard/oeschger cycles and the little ice age. Geophysical Monograph-American Geophysical Union 112, 35–58.

Boyer, T.P., Baranova, O.K., Coleman, C., Garcia, H.E., Grodsky, A., Locarnini, R.A., Mishonov, A.V., Paver, C.R., Reagan, J.R., Seidov, D., Smolyar, I.V., K, W., M M, Z., 2018. World ocean database 2018. In: Mishonov, A.V., Technical (Eds.). NOAA Atlas NESDIS, p. 87 (in preparation).

Broecker, W., Bond, G., Klas, M., Clark, E., McManus, J., 1992. Origin of the northern Atlantic's Heinrich events. Clim. Dynam. 6, 265–273. https://doi.org/10.1007/BF00193540.

Broecker, W.S., 1994. Massive iceberg discharges as triggers for global climate change. Nature 372, 421–424. https://doi.org/10.1038/372421a0.

Broecker, W.S., Peteet, D.M., Rind, D., 1985. Does the ocean–atmosphere system have more than one stable mode of operation? Nature 315, 21–26. https://doi.org/10.1038/315021a0.

Cacho, I., Grimalt, J.O., Canals, M., Sbaffi, L., Shackleton, N.J., Schönfeld, J., Zahn, R., 2001. Variability of the Western Mediterranean sea surface temperature during the last 25,000 years and its connection with the Northern Hemisphere climatic changes. Paleoceanography 16, 40–52. https://doi.org/10.1029/2000PA000502.

Cacho, I., Grimalt, J.O., Pelejero, C., Canals, M., Sierro, F.J., Flores, J.A., Shackleton, N., 1999. Dansgaard-oeschger and heinrich event imprints in Alboran Sea paleotemperatures. Paleoceanography 14, 698–705. https://doi.org/10.1029/1999PA900044.

Cacho, I., Grimalt, J.O., Sierro, F.J., Shackleton, N., Canals, M., 2000. Evidence for enhanced Mediterranean thermohaline circulation during rapid climatic coolings. Earth Planet Sci. Lett. 183, 417–429. https://doi.org/10.1016/S0012-821X(00)00296-X.

Capotondi, L., Girone, A., Lirer, F., Bergami, C., Verducci, M., Vallefuoco, M., Afferri, A., Ferraro, L., Pelosi, N., De Lange, G.J., 2016. Central Mediterranean Mid-Pleistocene paleoclimatic variability and its association with global climate. Palaeogeogr. Palaeoclimatol. Palaeoecol. 442, 72–83. https://doi.org/10.1016/j.palaeo.2015.11.009.

Casford, J., Rohling, E., Abu-Zied, R., Fontanier, C., Jorissen, F., Leng, M., Schmiedl, G., Thomson, J., 2003. A dynamic concept for eastern Mediterranean circulation and oxygenation during sapropel formation. Palaeogeogr. Palaeoclimatol. Palaeoecol. 190, 103–119. https://doi.org/10.1016/S0031-0182(02)00601-6.

Cheng, H., Edwards, R.L., Sinha, A., Spötl, C., Yi, L., Chen, S., Kelly, M., Kathayat, G., Wang, X., Li, X., 2016. The Asian monsoon over the past 640,000 years and ice age terminations. Nature 534, 640–646. https://doi.org/10.1038/nature18591.

Comas, M., Zahn, R., Klaus, A., 1996. Proc. Ocean Drill. Progr. Initial Rep. 161, 1023.

Coplen, T.B., Kendall, C., Hopple, J., 1983. Comparison of stable isotope reference samples. Nature 302, 236–238. https://doi.org/10.1038/302236a0.

Craig, H., 1957. Isotopic standards for carbon and oxygen and correction factors for mass-spectrometric analysis of carbon dioxide. Geochem. Cosmochim. Acta 12, 133–149. https://doi.org/10.1016/0016-7037(57)90024-8.

Dämmer, L.K., de Nooijer, L., van Sebille, E., Haak, J.G., Reichart, G.-J., 2020. Evaluation of oxygen isotopes and trace elements in planktonic foraminifera from the Mediterranean Sea as recorders of seawater oxygen isotopes and salinity. Clim. Past 16, 2401–2414. https://doi.org/10.5194/cp-16-2401-2020.

Daniault, N., Mercier, H., Lherminier, P., Sarafanov, A., Falina, A., Zunino, P., Pérez, F.F., Ríos, A.F., Ferron, B., Huck, T., 2016. The northern North Atlantic Ocean mean circulation in the early 21st century. Prog. Oceanogr. 146, 142–158. https://doi.org/10.1016/j.pocean.2016.06.007.

de Abreu, L., Abrantes, F.F., Shackleton, N.J., Tzedakis, P.C., McManus, J.F., Oppo, D.W., Hall, M.A., 2005. Ocean climate variability in the eastern North Atlantic during interglacial marine isotope stage 11: a partial analogue to the Holocene? Paleoceanography 20, 1–15. https://doi.org/10.1029/2004PA001091.

de Abreu, L., Shackleton, N.J., Schönfeld, J., Hall, M., Chapman, M., 2003. Millennial-scale oceanic climate variability off the Western Iberian margin during the last two glacial periods. Mar. Geol. 196, 1–20. https://doi.org/10.1016/S0025-3227(03)00046-X.

Desprat, S., Sánchez Goñi, M.F., Naughton, F., Turon, J.L., Duprat, J., Malaizé, B., Cortijo, E., Peypouquet, J.P., 2007. 25. Climate variability of the last five isotopic interglacials: direct land-sea-ice correlation from the multiproxy analysis of North-Western Iberian margin deep-sea cores. Dev. Quat. Sci. 375–386. https://doi.org/10.1016/S1571-0866(07)80050-9.

Desprat, S., Sánchez Goñi, M.F., Turon, J.L., McManus, J.F., Loutre, M.F., Duprat, J., Malaizé, B., Peyron, O., Peypouquet, J.P., 2005. Is vegetation responsible for glacial inception during periods of muted insolation changes? Quat. Sci. Rev. 24, 1361–1374. https://doi.org/10.1016/j.quascirev.2005.01.005.

Domínguez-Villar, D., Fairchild, I.J., Baker, A., Wang, X., Edwards, R.L., Cheng, H., 2009. Oxygen isotope precipitation anomaly in the North Atlantic region during the 8.2 ka event. Geology 37, 1095–1098. https://doi.org/10.1130/G30393A.1.

Droxler, A.W., Farrell, J.W., 2000. Marine isotope stage 11 (MIS 11): new insights for a warm future. Editorial. Global and Planetary Change 24, 1–5. https://doi.org/10.1016/S0921-8181(99)00065-X.

Ehlers, J., Gibbard, P.L., 2004. Quaternary Glaciations-Extent and Chronology: Part I: Europe. Elsevier.

Ehlers, J., Grube, A., Stephan, H.-J., Wansa, S., 2011. Pleistocene Glaciations of North Germany—new Results, Developments in Quaternary Sciences. Elsevier, pp. 149–162. https://doi.org/10.1016/B978-0-444-53447-7.00013-1.

Elderfield, H., Ferretti, P., Greaves, M., Crowhurst, S., McCave, I.N., Hodell, D., Piotrowski, A.M., 2012. Evolution of ocean temperature and ice volume through the mid-Pleistocene climate transition. Science 337, 704–709. https://doi.org/10.1126/science.1221294.

Elliot, M., Labeyrie, L., Duplessy, J.-C., 2002. Changes in North Atlantic deep-water formation associated with the Dansgaard–Oeschger temperature oscillations (60–10 ka). Quat. Sci. Rev. 21, 1153–1165. https://doi.org/10.1016/S0277-

3791(01)00137-8.
Emeis, K., Party, S.S., 1996. Paleoceanography and sapropel introduction. Proceedings of the Ocean Drilling Program, pp. 21–28 initial reports.
Emelianov, M., Font, J., Turiel, A., Millot, C., Solé, J., Poulain, P.-M., Julia, A., Vitria, M.-R., 2006. Transformation of levantine intermediate water tracked by MEDARGO floats in the western mediterranean. Ocean Sci. 2, 281–290. https://doi.org/10.5194/os-2-281-2006.
Erez, J., Luz, B., 1983. Experimental paleotemperature equation for planktonic foraminifera. Geochem. Cosmochim. Acta 47, 1025–1031. https://doi.org/10.1016/0016-7037(83)90232-6.
Eynaud, F., De Abreu, L., Voelker, A., Schönfeld, J., Salgueiro, E., Turon, J.L., Penaud, A., Toucanne, S., Naughton, F., Goñi, M.F.S., 2009. Position of the Polar Front along the western Iberian margin during key cold episodes of the last 45 ka. G-cubed 10. https://doi.org/10.1029/2009GC002398.
Font, J., Millot, C., Salas, J., Julià Brugues, A., Chic, Ó., 1998. The Drift of Modified Atlantic Water from the Alboran Sea to the Eastern Mediterranean.
Girone, A., Maiorano, P., Marino, M., Kucera, M., 2013. Calcareous plankton response to orbital and millennial-scale climate changes across the Middle Pleistocene in the western Mediterranean. Palaeogeogr. Palaeoclimatol. Palaeoecol. 392, 105–116. https://doi.org/10.1016/j.palaeo.2013.09.005.
González-Lanchas, A., Flores, J.-A., Sierro, F.J., Bárcena, M.Á., Rigual-Hernández, A.S., Oliveira, D., Azibeiro, L.A., Marino, M., Maiorano, P., Cortina, A., 2020. A new perspective of the Alboran Upwelling System reconstruction during the Marine Isotope Stage 11: a high-resolution coccolithophore record. Quat. Sci. Rev. 245, 106520. https://doi.org/10.1016/j.quascirev.2020.106520.
Goñi, M.S., Cacho, I., Turon, J.-L., Guiot, J., Sierro, F., Peypouquet, J., Grimalt, J., Shackleton, N., 2002. Synchroneity between marine and terrestrial responses to millennial scale climatic variability during the last glacial period in the Mediterranean region. Clim. Dynam. 19, 95–105. https://doi.org/10.1007/s00382-001-0212-x.
Grant, K., Grimm, R., Mikolajewicz, U., Marino, G., Ziegler, M., Rohling, E., 2016. The timing of Mediterranean sapropel deposition relative to insolation, sea-level and African monsoon changes. Quat. Sci. Rev. 140, 125–141. https://doi.org/10.1016/j.quascirev.2016.03.026.
Grant, K., Rohling, E., Bar-Matthews, M., Ayalon, A., Medina-Elizalde, M., Ramsey, C.B., Satow, C., Roberts, A., 2012. Rapid coupling between ice volume and polar temperature over the past 150,000 years. Nature 491, 744–747. https://doi.org/10.1038/nature11593.
Grant, K., Rohling, E., Ramsey, C.B., Cheng, H., Edwards, R., Florindo, F., Heslop, D., Marra, F., Roberts, A., Tamisiea, M.E., 2014. Sea-level variability over five glacial cycles. Nat. Commun. 5, 1–9. https://doi.org/10.1038/ncomms6076.
Grimm, R., Maier-Reimer, E., Mikolajewicz, U., Schmiedl, G., Müller-Navarra, K., Adloff, F., Grant, K.M., Ziegler, M., Lourens, L.J., Emeis, K.-C., 2015. Late glacial initiation of Holocene eastern Mediterranean sapropel formation. Nat. Commun. 6, 1–12. https://doi.org/10.1038/ncomms8099.
Grousset, F.E., Pujol, C., Labeyrie, L., Auffret, G., Boelaert, A., 2000. Were the North Atlantic Heinrich events triggered by the behavior of the European ice sheets? Geology 28, 123–126. https://doi.org/10.1130/0091-7613(2000)28<123:WTNAHE>2.0.CO;2.
Heinrich, H., 1988. Origin and consequences of cyclic ice rafting in the Northeast Atlantic Ocean during the past 130,000 years. Quat. Res. 29, 142–152. https://doi.org/10.1016/0033-5894(88)90057-9.
Hodell, D.A., Channeil, J.E.T., Curtis, J.H., Romero, O.E., Röhl, U., 2008. Onset of "hudson strait" heinrich events in the eastern north Atlantic at the end of the middle pleistocene transition (~640 ka)? Paleoceanography 23. https://doi.org/10.1029/2008PA001591.
Hodell, D.A., Martin-Garcia, G.M., Sierro, F.J., Mleneck-Vautravers, M., 2019. Impact of the channel outburst flood at 455 kyrs before present on north Atlantic climate. In: 20th Congress of the International Union for Quaternary Research (INQUA). Book of Abstracts.
Hodell, D.A., Nicholl, J.A., Bontognali, T.R., Danino, S., Dorador, J., Dowdeswell, J.A., Einsle, J., Kuhlmann, H., Martrat, B., Mleneck-Vautravers, M.J., 2017. Anatomy of Heinrich Layer 1 and its role in the last deglaciation. Paleoceanography 32, 284–303. https://doi.org/10.1002/2016PA003028.
Hughes, P., Woodward, J., Gibbard, P., 2007. Middle Pleistocene cold stage climates in the Mediterranean: new evidence from the glacial record. Earth Planet Sci. Lett. 253, 50–56. https://doi.org/10.1016/j.epsl.2006.10.019.
Hughes, P., Woodward, J., Van Calsteren, P., Thomas, L., 2011. The glacial history of the Dinaric Alps, Montenegro. Quat. Sci. Rev. 30, 3393–3412. https://doi.org/10.1016/j.quascirev.2011.08.016.
Hughes, P., Woodward, J., Van Calsteren, P., Thomas, L., Adamson, K., 2010. Pleistocene ice caps on the coastal mountains of the Adriatic Sea. Quat. Sci. Rev. 29, 3690–3708. https://doi.org/10.1016/j.quascirev.2010.06.032.
Huybers, P., 2006. Early Pleistocene glacial cycles and the integrated summer insolation forcing. Science 313, 508–511. https://doi.org/10.1126/science.1125249.
Ivy-Ochs, S., Kerschner, H., Reuther, A., Maisch, M., Sailer, R., Schaefer, J., Kubik, P.W., Synal, H., Schluchter, C., 2006. The timing of glacier advances in the northern European Alps based on surface exposure dating with cosmogenic^ 1^ 0Be,^ 2^ 6Al,^ 3^ 6Cl, and^ 2^ 1Ne. Spec. Pap. Geol. Soc. Am. 415, 43. https://doi.org/10.1130/2006.2415(04.
Jenkins, J.A., Williams, D.F., 1984. Nile water as a cause of eastern Mediterranean sapropel formation: evidence for and against. Mar. Micropaleontol. 8, 521–534.
Jiménez-Amat, P., Zahn, R., 2015. Offset timing of climate oscillations during the last two glacial-interglacial transitions connected with large-scale freshwater perturbation. Paleoceanography 30, 768–788. https://doi.org/10.1002/2014PA002710.
Jouzel, J., Masson-Delmotte, V., Cattani, O., Dreyfus, G., Falourd, S., Hoffmann, G., Minster, B., Nouet, J., Barnola, J.-M., Chappellaz, J., 2007. Orbital and millennial Antarctic climate variability over the past 800,000 years. Science 317, 793–796. https://doi.org/10.1126/science.1141038.
Kandiano, E.S., Bauch, H.A., Fahl, K., Helmke, J.P., Röhl, U., Pérez-Folgado, M., Cacho, I., 2012. The meridional temperature gradient in the eastern North Atlantic during MIS 11 and its link to the ocean-atmosphere system. Palaeogeogr. Palaeoclimatol. Palaeoecol. 333–334, 24–39. https://doi.org/10.1016/j.palaeo.2012.03.005.
Kim, S.-T., Coplen, T.B., Horita, J., 2015. Normalization of stable isotope data for carbonate minerals: implementation of IUPAC guidelines. Geochem. Cosmochim. Acta 158, 276–289. https://doi.org/10.1016/j.gca.2015.02.011.
Kim, S.T., O'Neil, J.R., 1997. Equilibrium and nonequilibrium oxygen isotope effects in synthetic carbonates. Geochem. Cosmochim. Acta 61, 3461–3475. https://doi.org/10.1016/S0016-7037(97)00169-5.
Konijnendijk, T.Y.M., Ziegler, M., Lourens, L.J., 2014. Chronological constraints on Pleistocene sapropel depositions from high-resolution geochemical records of ODP sites 967 and 968. Newsl. Stratigr. 47, 263–282. https://doi.org/10.1127/0078-0421/2014/0047.
Koutsodendris, A., Kousis, I., Peyron, O., Wagner, B., Pross, J., 2019. The Marine Isotope Stage 12 pollen record from Lake Ohrid (SE Europe): investigating short-term climate change under extreme glacial conditions. Quat. Sci. Rev. 221, 105873. https://doi.org/10.1016/j.quascirev.2019.105873.
Kucera, M., Weinelt, M., Kiefer, T., Pflaumann, U., Hayes, A., Weinelt, M., Chen, M.-T., Mix, A.C., Barrows, T.T., Cortijo, E., 2005. Reconstruction of sea-surface temperatures from assemblages of planktonic foraminifera: multi-technique approach based on geographically constrained calibration data sets and its application to glacial Atlantic and Pacific Oceans. Quat. Sci. Rev. 24, 951–998. https://doi.org/10.1016/j.quascirev.2004.07.014.
Lacombe, H., 1981. To the water and energy fluxes. Oceanol. Acta 4, 247–255.
Lane Serff, G.F., Rohling, E.J., Bryden, H.L., Charnock, H., 1997. Postglacial connection of the Black Sea to the Mediterranean and its relation to the timing of sapropel formation. Paleoceanography 12, 169–174. https://doi.org/10.1029/96PA03934.
Langereis, C., Dekkers, M., De Lange, G., Paterne, M., Van Santvoort, P., 1997. Magnetostratigraphy and astronomical calibration of the last 1.1 Myr from an eastern Mediterranean piston core and dating of short events in the Brunhes. Geophys. J. Int. 129, 75–94. https://doi.org/10.1111/j.1365-246X.1997.tb00938.x.
Lea, D.W., Martin, P.A., Pak, D.K., Spero, H.J., 2002. Reconstructing a 350 ky history of sea level using planktonic Mg/Ca and oxygen isotope records from a Cocos Ridge core. Quat. Sci. Rev. 21, 283–293. https://doi.org/10.1016/S0277-3791(01)00081-6.
LeGrande, A.N., Schmidt, G.A., 2006. Global gridded data set of the oxygen isotopic composition in seawater. Geophys. Res. Lett. 33. https://doi.org/10.1029/2006GL026011.
Leicher, N., Zanchetta, G., Sulpizio, R., Giaccio, B., Wagner, B., Nomade, S., Francke, A., Carlo, P.D., 2016. First tephrostratigraphic results of the DEEP site record from Lake Ohrid (Macedonia and Albania). Biogeosciences 13, 2151–2178. https://doi.org/10.5194/bg-13-2151-2016.
Leontaritis, A., Kouli, K., Pavlopoulos, K., 2020. The glacial history of Greece: a comprehensive review. Mediterranean Geoscience Reviews 2, 65–90. https://doi.org/10.1007/s42990-020-00021-w.
Lisiecki, L.E., Raymo, M.E., 2005. A Pliocene-Pleistocene stack of 57 globally distributed benthic δ18O records. Paleoceanography 20, 1. https://doi.org/10.1029/2004PA001071.
Lourens, L.J., 2004. Revised tuning of Ocean Drilling Program Site 964 and KC01B (Mediterranean) and implications for the δ18O, tephra, calcareous nannofossil, and geomagnetic reversal chronologies of the past 1.1 Myr. Paleoceanography 19, 3011–3020. https://doi.org/10.1029/2003PA000997. PA3010.
Lourens, L.J., Antonarakou, A., Hilgen, F., Van Hoof, A., Vergnaud-Grazzini, C., Zachariasse, W., 1996. Evaluation of the plio-pleistocene astronomical timescale. Paleoceanography 11, 391–413. https://doi.org/10.1029/96PA01125.
Loutre, M.F., 2003. Clues from MIS 11 to predict the future climate - a modelling point of view. Earth Planet Sci. Lett. 212, 213–224. https://doi.org/10.1016/S0012-821X(03)00235-8.
Macias, D., Cózar, A., Garcia-Gorriz, E., González-Fernández, D., Stips, A., 2019. Surface water circulation develops seasonally changing patterns of floating litter accumulation in the Mediterranean Sea. A modelling approach. Mar. Pollut. Bull. 149, 110619. https://doi.org/10.1016/j.marpolbul.2019.110619.
Maiorano, P., Girone, A., Marino, M., Kucera, M., Pelosi, N., 2016. Sea surface water variability during the Mid-Brunhes inferred from calcareous plankton in the western Mediterranean (ODP Site 975). Palaeogeogr. Palaeoclimatol. Palaeoecol. 459, 229–248. https://doi.org/10.1016/j.palaeo.2016.07.006.
Major, C., Ryan, W., Lericolais, G., Hajdas, I., 2002. Constraints on Black Sea outflow to the Sea of Marmara during the last glacial–interglacial transition. Mar. Geol. 190, 19–34. https://doi.org/10.1016/S0025-3227(02)00340-7.
Major, C.O., Goldstein, S.L., Ryan, W.B., Lericolais, G., Piotrowski, A.M., Hajdas, I., 2006. The co-evolution of Black Sea level and composition through the last deglaciation and its paleoclimatic significance. Quat. Sci. Rev. 25, 2031–2047. https://doi.org/10.1016/j.quascirev.2006.01.032.
Malmgren, B.A., Kucera, M., Nyberg, J., Waelbrocck, C., 2001. Comparison of statistical and artificial neural network techniques for estimating past sea surface temperatures from planktonic foraminifer census data. Paleoceanography 16, 520–530. https://doi.org/10.1029/2000PA000562.

Mangerud, J., Jakobsson, M., Alexanderson, H., Astakhov, V., Clarke, G.K., Henriksen, M., Hjort, C., Krinner, G., Lunkka, J.-P., Möller, P., 2004. Ice-dammed lakes and rerouting of the drainage of northern Eurasia during the Last Glaciation. Quat. Sci. Rev. 23, 1313–1332. https://doi.org/10.1016/j.quascirev.2003.12.009.

Marino, M., Girone, A., Maiorano, P., Di Renzo, R., Piscitelli, A., Flores, J.A., 2018. Calcareous plankton and the mid-Brunhes climate variability in the Alboran Sea (ODP Site 977). Palaeogeogr. Palaeoclimatol. Palaeoecol. 508, 91–106. https://doi.org/10.1016/j.palaeo.2018.07.023.

Marino, M., Maiorano, P., Tarantino, F., Voelker, A., Capotondi, L., Girone, A., Lirer, F., Flores, J.A., Naafs, B.D.A., 2014. Coccolithophores as proxy of seawater changes at orbital-to-millennial scale during middle Pleistocene Marine Isotope Stages 14–9 in North Atlantic core MD01-2446. Paleoceanography 29, 518–532. https://doi.org/10.1002/2013PA002574.

Marjanac, T., Marjanac, L., 2016. The extent of middle Pleistocene ice cap in the coastal Dinaric Mountains of Croatia. Quat. Res. 85, 445–455. https://doi.org/10.1016/j.yqres.2016.03.006.

Martinez-Lamas, R., Toucanne, S., Debret, M., Riboulot, V., Deloffre, J., Boissier, A., Cheron, S., Pitel, M., Bayon, G., Giosan, L., 2020. Linking Danube River activity to Alpine Ice-Sheet fluctuations during the last glacial (ca. 33–17 ka BP): insights into the continental signature of Heinrich Stadials. Quat. Sci. Rev. 229, 106136. https://doi.org/10.1016/j.quascirev.2019.106136.

Martrat, B., Grimalt, J.O., Lopez-Martinez, C., Cacho, I., Sierro, F.J., Flores, J.A., Zahn, R., Canals, M., Curtis, J.H., Hodell, D.A., 2004. Abrupt temperature changes in the Western Mediterranean over the past 250,000 years. Science 306, 1762–1765. https://doi.org/10.1126/science.1101706.

Martrat, B., Grimalt, J.O., Shackleton, N.J., De Abreu, L., Hutterli, M.A., Stocker, T.F., 2007. Four climate cycles of recurring deep and surface water destabilizations on the Iberian margin. Science 317, 502–507. https://doi.org/10.1126/science.1139994.

Maselli, V., Trincardi, F., Asioli, A., Ceregato, A., Rizzetto, F., Taviani, M., 2014. Delta growth and river valleys: the influence of climate and sea level changes on the South Adriatic shelf (Mediterranean Sea). Quat. Sci. Rev. 99, 146–163. https://doi.org/10.1016/j.quascirev.2014.06.014.

Matthiesen, S., Haines, K., 2003. A hydraulic box model study of the Mediterranean response to postglacial sea-level rise. Paleoceanography 18. https://doi.org/10.1029/2003PA000880.

McManus, J., Oppo, D., Cullen, J., Healey, S., 2003. Marine isotope stage 11 (MIS 11): analog for holocene and future climate? Geophys. Monogr. 69–85. https://doi.org/10.1029/137GM06.

McManus, J.F., Francois, R., Gherardi, J.-M., Keigwin, L.D., Brown-Leger, S., 2004. Collapse and rapid resumption of Atlantic meridional circulation linked to deglacial climate changes. Nature 428, 834–837. https://doi.org/10.1038/nature02494.

McManus, J.F., Oppo, D.W., Cullen, J.L., 1999. A 0.5-million-year record of millennial-scale climate variability in the North Atlantic. Science 283, 971–975.

Millot, C., 1999. Circulation in the western Mediterranean sea. J. Mar. Syst. 20, 423–442. https://doi.org/10.1016/S0924-7963(98)00078-5.

Millot, C., Taupier-Letage, I., 2005. Circulation in the Mediterranean Sea, the Mediterranean Sea. Springer, pp. 29–66. https://doi.org/10.1007/b107143.

Monegato, G., Ravazzi, C., Donegana, M., Pini, R., Calderoni, G., Wick, L., 2007. Evidence of a two-fold glacial advance during the last glacial maximum in the Tagliamento end moraine system (eastern Alps). Quat. Res. 68, 284–302.

Myers, P.G., Haines, K., Rohling, E.J., 1998. Modeling the paleocirculation of the Mediterranean: the last glacial maximum and the Holocene with emphasis on the formation of sapropel S 1. Paleoceanography 13, 586–606.

Naafs, B.D.A., Hefter, J., Ferretti, P., Stein, R., Haug, G.H., 2011. Sea surface temperatures did not control the first occurrence of Hudson Strait Heinrich Events during MIS 16. Paleoceanography 26. https://doi.org/10.1029/2011PA002135.

Naafs, B.D.A., Hefter, J., Stein, R., 2014. Dansgaard-Oeschger forcing of sea surface temperature variability in the midlatitude North Atlantic between 500 and 400ka (MIS 12). Paleoceanography 29, 1024–1030. https://doi.org/10.1002/2014PA002697.

Naughton, F., Goñi, M.S., Kageyama, M., Bard, E., Duprat, J., Cortijo, E., Desprat, S., Malaizé, B., Joly, C., Rostek, F., 2009. Wet to dry climatic trend in north-western Iberia within Heinrich events. Earth Planet Sci. Lett. 284, 329–342. https://doi.org/10.1016/j.epsl.2009.05.001.

Oppo, D., McManus, J., Cullen, J., 1998. Abrupt climate events 500,000 to 340,000 years ago: evidence from subpolar North Atlantic sediments. Science 279, 1335–1338.

Palumbo, E., Flores, J.A., Perugia, C., Petrillo, Z., Voelker, A.H.L., Amore, F.O., 2013. Millennial scale coccolithophore paleoproductivity and surface water changes between 445 and 360ka (Marine Isotope Stages 12/11) in the Northeast Atlantic. Palaeogeogr. Palaeoclimatol. Palaeoecol. 383–384, 27–41. https://doi.org/10.1016/j.palaeo.2013.04.024.

Paterne, M., Kallel, N., Labeyrie, L., Vautravers, M., Duplessy, J.C., Rossignol-Strick, M., Cortijo, E., Arnold, M., Fontugne, M., 1999. Hydrological relationship between the north atlantic ocean and the Mediterranean sea during the past 15 - 75 kyr. Paleoceanography 14, 626–638. https://doi.org/10.1029/1998PA900022.

Peck, V.L., Hall, I.R., Zahn, R., Elderfield, H., Grousset, F., Hemming, S., Scourse, J., 2006. High resolution evidence for linkages between NW European ice sheet instability and Atlantic Meridional Overturning Circulation. Earth Planet Sci. Lett. 243, 476–488. https://doi.org/10.1016/j.epsl.2005.12.023.

Peck, V.L., Hall, I.R., Zahn, R., Scourse, J., 2007. Progressive reduction in NE Atlantic intermediate water ventilation prior to Heinrich events: response to NW European ice sheet instabilities? G-cubed 8. https://doi.org/10.1029/2006GC001321.

Peliz, Á., Dubert, J., Santos, A.M.P., Oliveira, P.B., Le Cann, B., 2005. Winter upper ocean circulation in the western iberian basin—fronts, eddies and poleward flows: an overview. Deep-Sea Res. Part I Oceanogr. Res. Pap. 52, 621–646. https://doi.org/10.1016/j.dsr.2004.11.005.

Pérez-Folgado, M., Sierro, F.J., Flores, J.A., Cacho, I., Grimalt, J.O., Zahn, R., Shackleton, N., 2003. Western Mediterranean planktonic foraminifera events and millennial climatic variability during the last 70 kyr. Mar. Micropaleontol. 48, 49–70. https://doi.org/10.1016/S0377-8398(02)00160-3.

Pérez-Folgado, M., Sierro, F.J., Flores, J.A., Grimalt, J.O., Zahn, R., 2004. Paleoclimatic variations in foraminifer assemblages from the Alboran Sea (western mediterranean) during the last 150 ka in ODP site 977. Mar. Geol. 212, 113–131. https://doi.org/10.1016/j.margeo.2004.08.002.

Pierre, C., 1999. The oxygen and carbon isotope distribution in the Mediterranean water masses. Mar. Geol. 153 (1–4), 41–55. https://doi.org/10.1016/S0025-3227(98)00090-5.

Poli, M., Thunell, R., Rio, D., 2000. Millennial-scale changes in north Atlantic deep water circulation during marine isotope stages 11 and 12: linkage to antarctic climate. Geology 28, 807–810. https://doi.org/10.1130/0091-7613(2000)28<807:MCINAD>2.0.CO;2.

Pross, J., Koutsodendris, A., Christanis, K., Fischer, T., Fletcher, W.J., Hardiman, M., Kalaitzidis, S., Knipping, M., Kotthoff, U., Milner, A.M., 2015. The 1.35-Ma-long terrestrial climate archive of Tenaghi Philippon, northeastern Greece: evolution, exploration, and perspectives for future research. Newsl. Stratigr. 48, 253–276. https://doi.org/10.1127/nos/2015/0063.

Railsback, L.B., Gibbard, P.L., Head, M.J., Voarintsoa, N.R.G., Toucanne, S., 2015. An optimized scheme of lettered marine isotope substages for the last 1.0 million years, and the climatostratigraphic nature of isotope stages and substages. Quat. Sci. Rev. 111, 94–106. https://doi.org/10.1016/j.quascirev.2015.01.012.

Ravazzi, C., Pini, R., Badino, F., De Amicis, M., Londeix, L., Reimer, P.J., 2014. The latest LGM culmination of the Garda Glacier (Italian Alps) and the onset of glacial termination. Age of glacial collapse and vegetation chronosequence. Quat. Sci. Rev. 105, 26–47. https://doi.org/10.1016/j.quascirev.2014.09.014.

Regattieri, E., Giaccio, B., Galli, P., Nomade, S., Peronace, E., Messina, P., Sposato, A., Boschi, C., Gemelli, M., 2016. A multi-proxy record of MIS 11–12 deglaciation and glacial MIS 12 instability from the Sulmona basin (central Italy). Quat. Sci. Rev. 132, 129–145. https://doi.org/10.1016/j.quascirev.2015.11.015.

Rodrigues, T., Alonso-García, M., Hodell, D.A., Rufino, M., Naughton, F., Grimalt, J.O., Voelker, A.H.L., Abrantes, F., 2017. A 1-Ma record of sea surface temperature and extreme cooling events in the North Atlantic: a perspective from the Iberian Margin. Quat. Sci. Rev. 172, 118–130. https://doi.org/10.1016/j.quascirev.2017.07.004.

Rodrigues, T., Voelker, A.H.L., Grimalt, J.O., Abrantes, F., Naughton, F., 2011. Iberian Margin sea surface temperature during MIS 15 to 9 (580-300 ka): glacial suborbital variability versus interglacial stability. Paleoceanography 26. https://doi.org/10.1029/2010PA001927.

Rogerson, M., Cacho, I., Jimenez-Espejo, F., Reguera, M.I., Sierro, F.J., Martinez-Ruiz, F., Frigola, J., Canals, M., 2008. A dynamic explanation for the origin of the western Mediterranean organic-rich layers. G-cubed 9. https://doi.org/10.1029/2007GC001936.

Rogerson, M., Colmenero-Hidalgo, E., Levine, R.C., Rohling, E.J., Voelker, A.H.L., Bigg, G.R., Schönfeld, J., Cacho, I., Sierro, F.J., Löwemark, L., Reguera, M.I., De Abreu, L., Garrick, K., 2010. Enhanced Mediterranean-Atlantic exchange during Atlantic freshening phases. G-cubed 11. https://doi.org/10.1029/2009GC002931.

Rohling, E., Foster, G.L., Grant, K., Marino, G., Roberts, A., Tamisiea, M.E., Williams, F., 2014. Sea-level and deep-sea-temperature variability over the past 5.3 million years. Nature 508, 477–482. https://doi.org/10.1038/nature13230.

Rohling, E., Marino, G., Grant, K., 2015. Mediterranean climate and oceanography, and the periodic development of anoxic events (sapropels). Earth Sci. Rev. 143, 62–97. https://doi.org/10.1016/j.earscirev.2015.01.008.

Rohling, E., Sprovieri, M., Cane, T., Casford, J.S., Cooke, S., Bouloubassi, I., Emeis, K., Schiebel, R., Rogerson, M., Hayes, A., 2004. Reconstructing past planktic foraminiferal habitats using stable isotope data: a case history for Mediterranean sapropel S5. Mar. Micropaleontol. 50, 89–123. https://doi.org/10.1016/S0377-8398(03)00068-9.

Rohling, E.J., 1994. Review and new aspects concerning the formation of eastern Mediterranean sapropels. Mar. Geol. 122, 1–28. https://doi.org/10.1016/0025-3227(94)90202-X.

Rohling, E.J., 1999. Environmental control on Mediterranean salinity and δ18O. Paleoceanography 14, 706–715. https://doi.org/10.1029/1999PA900042.

Rohling, E.J., 2007. Progress in paleosalinity: overview and presentation of a new approach. Paleoceanography 22. https://doi.org/10.1029/2007PA001437.

Rohling, E.J., Fenton, M.J.J.F., Jorissen, F.J., Bertrand, P., Ganssen, G., Caulet, J.P., 1998a. Magnitudes of sea-level lowstands of the past 500,000 years. Nature 394, 162.

Rohling, E.J., Hayes, A., De Rijk, S., Kroon, D., Zachariasse, W.J., Eisma, D., 1998b. Abrupt cold spells in the northwest Mediterranean. Paleoceanography 13, 316–322. https://doi.org/10.1029/98PA00671.

Rossato, S., Mozzi, P., 2016. Inferring LGM sedimentary and climatic changes in the southern Eastern Alps foreland through the analysis of a 14C ages database (Brenta megafan, Italy). Quat. Sci. Rev. 148, 115–127. https://doi.org/10.1016/j.quascirev.2016.07.013.

Rossignol-Strick, M., 1985. Mediterranean Quaternary sapropels, an immediate response of the African monsoon to variation of insolation. Palaeogeogr.

Palaeoclimatol. Palaeoecol. 49, 237–263. https://doi.org/10.1016/0031-0182(85)90056-2.
Rossignol-Strick, M., Nesteroff, W., Olive, P., Vergnaud-Grazzini, C., 1982. After the deluge: Mediterranean stagnation and sapropel formation. Nature 295, 105–110. https://doi.org/10.1038/295105a0.
Rossignol-Strick, M., Paterne, M., 1999. A synthetic pollen record of the eastern Mediterranean sapropels of the last 1 Ma: implications for the time-scale and formation of sapropels. Mar. Geol. 153, 221–237. https://doi.org/10.1016/S0025-3227(98)00080-2.
Ryan, W.B., Major, C.O., Lericolais, G., Goldstein, S.L., 2003. Catastrophic flooding of the Black sea. Annu. Rev. Earth Planet Sci. 31, 525–554. https://doi.org/10.1146/annurev.earth.31.100901.141249.
Ryan, W.B., Pitman III, W.C., Major, C.O., Shimkus, K., Moskalenko, V., Jones, G.A., Dimitrov, P., Gorür, N., Sakinç, M., Yüce, H., 1997. An abrupt drowning of the Black Sea shelf. Mar. Geol. 138, 119–126. https://doi.org/10.1016/S0025-3227(97)00007-8.
Sadori, L., Koutsodendris, A., Panagiotopoulos, K., Masi, A., Bertini, A., Combourieu-Nebout, N., Francke, A., Kouli, K., Joannin, S., Mercuri, A.M., 2016. Pollen-based paleoenvironmental and paleoclimatic change at Lake Ohrid (south-eastern Europe) during the past 500 ka. Biogeosciences 13, 1423–1437. https://doi.org/10.5194/bg-13-1423-2016.
Schmidt, G., 1999. Global seawater oxygen-18 database. http://data.giss.nasa.gov/o18data/.
Seguinot, J., Ivy-Ochs, S., Jouvet, G., Huss, M., Funk, M., Preusser, F., 2018. Modelling last glacial cycle ice dynamics in the Alps. Cryosphere 12, 3265–3285. https://doi.org/10.5194/tc-12-3265-2018.
Sierro, F.J., Hodell, D.A., Andersen, N., Azibeiro, L.A., Jimenez-Espejo, F.J., Bahr, A., Flores, J.A., Ausin, B., Rogerson, M., Lozano-Luz, R., 2020. Mediterranean overflow over the last 250 kyr: freshwater forcing from the tropics to the ice sheets. Paleoceanography and Paleoclimatology 35, e2020PA003931. https://doi.org/10.1029/2020PA003931.
Sierro, F.J., Hodell, D.A., Curtis, J.H., Flores, J.A., Reguera, I., Colmenero-Hidalgo, E., Bárcena, M.A., Grimalt, J.O., Cacho, I., Frigola, J., Canals, M., 2005. Impact of iceberg melting on Mediterranean thermohaline circulation during Heinrich events. Paleoceanography 20, 1–13. https://doi.org/10.1029/2004PA001051.
Sosdian, S., Rosenthal, Y., 2009. Deep-sea temperature and ice volume changes across the Pliocene-Pleistocene climate transitions. Science 325, 306–310. https://doi.org/10.1126/science.1169938.
Soulet, G., Delaygue, G., Vallet-Coulomb, C., Böttcher, M., Sonzogni, C., Lericolais, G., Bard, E., 2010. Glacial hydrologic conditions in the Black Sea reconstructed using geochemical pore water profiles. Earth Planet Sci. Lett. 296, 57–66. https://doi.org/10.1016/j.epsl.2010.04.045.
Soulet, G., Ménot, G., Bayon, G., Rostek, F., Ponzevera, E., Toucanne, S., Lericolais, G., Bard, E., 2013. Abrupt drainage cycles of the fennoscandian ice sheet. Proc. Natl. Acad. Sci. Unit. States Am. 110, 6682–6687. https://doi.org/10.1073/pnas.1214676110.
Sperling, M., Schmiedl, G., Hemleben, C., Emeis, K., Erlenkeuser, H., Grootes, P., 2003. Black sea impact on the formation of eastern mediterranean sapropel S1? Evidence from the Marmara Sea. Palaeogeogr. Palaeoclimatol. Palaeoecol. 190, 9–21. https://doi.org/10.1016/S0031-0182(02)00596-5.
Stein, R., Hefter, J., Grützner, J., Voelker, A., David A Naafs, B., 2009. Variability of surface water characteristics and heinrich-iike events in the pleistocene mid-latitude North Atlantic Ocean: biomarker and XRD records from iodp site U1313 (MIS 16-9). Paleoceanography 24. https://doi.org/10.1029/2008PA001639.
Toucanne, S., Soulet, G., Vázquez Riveiros, N., Boswell, S.M., Dennielou, B., Waelbroeck, C., Bayon, G., Mojtahid, M., Bosq, M., Sabine, M., 2021. the North atlantic glacial eastern boundary current as a key driver for ice-sheet—AMOC interactions and climate instability. Paleoceanography and Paleoclimatology 36, e2020PA004068. https://doi.org/10.1029/2020PA004068.
Toucanne, S., Zaragosi, S., Bourillet, J.-F., Gibbard, P., Eynaud, F., Giraudeau, J., Turon, J., Cremer, M., Cortijo, E., Martinez, P., 2009. A 1.2 Ma record of glaciation and fluvial discharge from the West European Atlantic margin. Quat. Sci. Rev. 28, 2974–2981. https://doi.org/10.1016/j.quascirev.2009.08.003.
Tudryn, A., Leroy, S.A., Toucanne, S., Gibert-Brunet, E., Tucholka, P., Lavrushin, Y.A., Dufaure, O., Miska, S., Bayon, G., 2016. The Ponto-Caspian basin as a final trap for southeastern Scandinavian Ice-Sheet meltwater. Quat. Sci. Rev. 148, 29–43. https://doi.org/10.1016/j.quascirev.2016.06.019.
Tzedakis, P., Crucifix, M., Mitsui, T., Wolff, E.W., 2017. A simple rule to determine which insolation cycles lead to interglacials. Nature 542, 427–432. https://doi.org/10.1038/nature21364.
Tzedakis, P., Hooghiemstra, H., Pälike, H., 2006. The last 1.35 million years at Tenaghi Philippon: revised chronostratigraphy and long-term vegetation trends. Quat. Sci. Rev. 25, 3416–3430.
Tzedakis, P., Wolff, E., Skinner, L., Brovkin, V., Hodell, D., McManus, J.F., Raynaud, D., 2012. Can we predict the duration of an interglacial? Clim. Past 8, 1473–1485. https://doi.org/10.5194/cp-8-1473-2012.
Tzedakis, P.C., 2010. The MIS 11 - MIS 1 analogy, southern European vegetation, atmospheric methane and the "early anthropogenic hypothesis. Clim. Past 6, 131–144. https://doi.org/10.5194/cp-6-131-2010.
Vidal, L., Labeyrie, L., Cortijo, E., Arnold, M., Duplessy, J., Michel, E., Becque, S., Van Weering, T., 1997. Evidence for changes in the north atlantic deep water linked to meltwater surges during the heinrich events. Earth Planet Sci. Lett. 146, 13–27. https://doi.org/10.1016/S0012-821X(96)00192-6.
Vidal, L., Menot, G., Joly, C., Bruneton, H., Rostek, F., Çağatay, M., Major, C., Bard, E., 2010. Hydrology in the Sea of Marmara during the last 23 ka: implications for timing of Black Sea connections and sapropel deposition. Paleoceanography 25. https://doi.org/10.1029/2009PA001735.
Voelker, A., De Abreu, L., Schönfeld, J., Erlenkeuser, H., Abrantes, F., 2009. Hydrographic conditions along the western Iberian margin during marine isotope stage 2. G-cubed 10. https://doi.org/10.1029/2009GC002605.
Voelker, A.H., Colman, A., Olack, G., Waniek, J.J., Hodell, D., 2015. Oxygen and hydrogen isotope signatures of Northeast Atlantic water masses. Deep Sea Res. Part II Top. Stud. Oceanogr. 116, 89–106. https://doi.org/10.1016/j.dsr2.2014.11.006.
Voelker, A.H., de Abreu, L., 2011. A review of abrupt climate change events in the Northeastern Atlantic Ocean (Iberian Margin): latitudinal, longitudinal, and vertical gradients. Abrupt Climate Change: Mechanisms, Patterns, and Impacts 193, 15–37. https://doi.org/10.5194/cp-6-531-2010.
Voelker, A.H.L., Rodrigues, T., Billups, K., Oppo, D., McManus, J., Stein, R., Hefter, J., Grimalt, J.O., 2010. Variations in mid-latitude North Atlantic surface water properties during the mid-Brunhes (MIS 9-14) and their implications for the thermohaline circulation. Clim. Past 6, 531–552. https://doi.org/10.5194/cp-6-531-2010.
Wang, P., Tian, J., Lourens, L.J., 2010. Obscuring of long eccentricity cyclicity in Pleistocene oceanic carbon isotope records. Earth Planet Sci. Lett. 290, 319–330. https://doi.org/10.1016/j.epsl.2009.12.028.
Wehausen, R., Brumsack, H.-J., 2000. Chemical cycles in Pliocene sapropel-bearing and sapropel-barren eastern Mediterranean sediments. Palaeogeogr. Palaeoclimatol. Palaeoecol 158, 325–352. https://doi.org/10.1016/S0031-0182(00)00057-2.
WOA, 1998. World ocean atlas 1998, version 2. In: Tech. rep., NationalOceanog Raphic Data Center. Silver Spring, Maryland. http://www.nodc.-noaa.gov/oc5/woa98.html.
Woodward, J., Hamlin, R., Macklin, M., Hughes, P., Lewin, J., 2008. Glacial activity and catchment dynamics in northwest Greece: long-term river behaviour and the slackwater sediment record for the last glacial to interglacial transition. Geomorphology 101, 44–67. https://doi.org/10.1016/j.geomorph.2008.05.018.
Zweng, M.M., Reagan, J.R., Seidov, D., Boyer, T.P., Locarnini, R.A., Garcia, H.E., Mishonov, A.V., Baranova, O.K., Weathers, K., Paver, C.R., Smolyar, I.V., 2018. World ocean atlas 2018, volume 2: salinity. In: Mishonov Technical, A. (Ed.), NOAA Atlas NESDIS, vol. 82, p. 50.